STOCHASTIC ESTIMATION OF THE STRUCTURE OF TURBULENT FIELDS

Ronald J. Adrian
Department of Theoretical and Applied Mechanics
University of Illinois
Urbana, Illinois, USA 61801

ABSTRACT

The stochastic estimation method educes structure by approximating an average field in terms of event data that are given. The estimated fields satisfy the continuity equation, and they possess the correct scales of length and/or time. The fundamental concepts of general stochastic estimation and the specific application of this technique to the estimation of conditional averages are discussed. Linear stochastic estimation of random fields and of their conditional averages is developed as the principal tool, and its accuracy is demonstrated. The linear stochastic estimate is expressible in terms of second order correlation functions between the given event data and the quantity being estimated. This establishes a simple link between conditional averages, the coherent structure that they represent and correlation functions. The related problems of selecting events and interpreting the estimates that result from a given set of events are explored by considering events of increasing complexity: single-point vectors, two-point vectors, local deformation tensors, multi-point vectors, space-time vectors, and space-wave-number events. General kinematic and statistical properties are derived, and stochastically estimated structures from various types of turbulent flows are described and related to the underlying coherent structures.

1. INTRODUCTION

1.1 Estimation of random processes

In general, stochastic estimation deals with the estimation of one random variable, say $\mathbf{y}$, in terms of a set of other variables $E_1,...,E_N$ about which some information is

known. We shall denote this set as the *data vector* $\mathbf{E}= (E1,...,EN)$. The data vector $\mathbf{E}$ may or may not contain all of the variables that affect $\mathbf{y}$, and it may even contain some that are irrelevant, but in any case it represents a list of the available information that is thought to be important. The problem is to find a function $\mathbf{F}(\mathbf{E})$ that approximates $\mathbf{y}$ in some sense. Estimating a quantity in terms of other parameters is, of course, ubiquitous in engineering and science, and for this reason stochastic estimation is a well known process, especially in communications and information theory-related disciplines [Papoulis 1984], [Deutsch 1965]. It also arises routinely in our daily lives, as for example when one makes the decision to walk across a street based on an estimate of the arrival time of the approaching automobiles in terms of visual image data and engine sounds, or when one estimates the future weather in terms of current conditions.

A common element in stochastic estimation methods is that they employ information on the relationships between the variables that is based largely on empirical experience as embodied in a statistical relationship between $\mathbf{y}$ and $\mathbf{E}$. This should be contrasted to mathematical models in which empirical information is ultimately condensed into the form of the governing differential equations and the coefficients contained therein. Full statistical information is contained in the joint probability density function

$$f_{\mathbf{y},\mathbf{E}}(\psi,\varepsilon)d\psi d\varepsilon = \Pr ob\{\psi \le \mathbf{y} < \psi + d\psi \quad and \quad \varepsilon \le \mathbf{E} < \varepsilon + d\varepsilon\} \tag{1.1}$$

where ψ and ε are dummy variables in the *pdf*. The conditional probability density of $\mathbf{y}$ given $\mathbf{E}$ is defined by

$$f_{\mathbf{y}|\mathbf{E}}(\psi \mid \varepsilon) = f_{\mathbf{y},\mathbf{E}}(\psi,\varepsilon) / f_{\mathbf{E}}(\varepsilon) \tag{1.2}$$

Consider the plot of y versus E in Figure 1.1, where both are taken to be scalars for purposes of illustration. There are two widely used methods for estimating y in terms of E. Firstly, for a given value of E, the *maximum likelihood estimate* of y is defined as the most probable value, i.e that value y_{max} at which $f_{\mathbf{y}|\mathbf{E}}$ is a maximum. It is natural to think in terms of estimates which represent the most likely result given the available data.

The second method is *conditional averaging*. The conditional average of y given E is defined as the centroid of the conditional probability

$$\langle \mathbf{y} \mid \mathbf{E} \rangle = \int \psi f_{\mathbf{y}|\mathbf{E}}(\psi \mid \varepsilon) d\psi. \tag{1.3}$$

It represents the mean value of y found by averaging over the realizations in which the event E occurs. The degree to which $<y \mid E>$ is a good estimate of the state of y given E depends upon the dispersion of y around $<y \mid E>$. As with unconditional probability distributions, accuracy can be represented by the root mean square value of the conditional distribution:

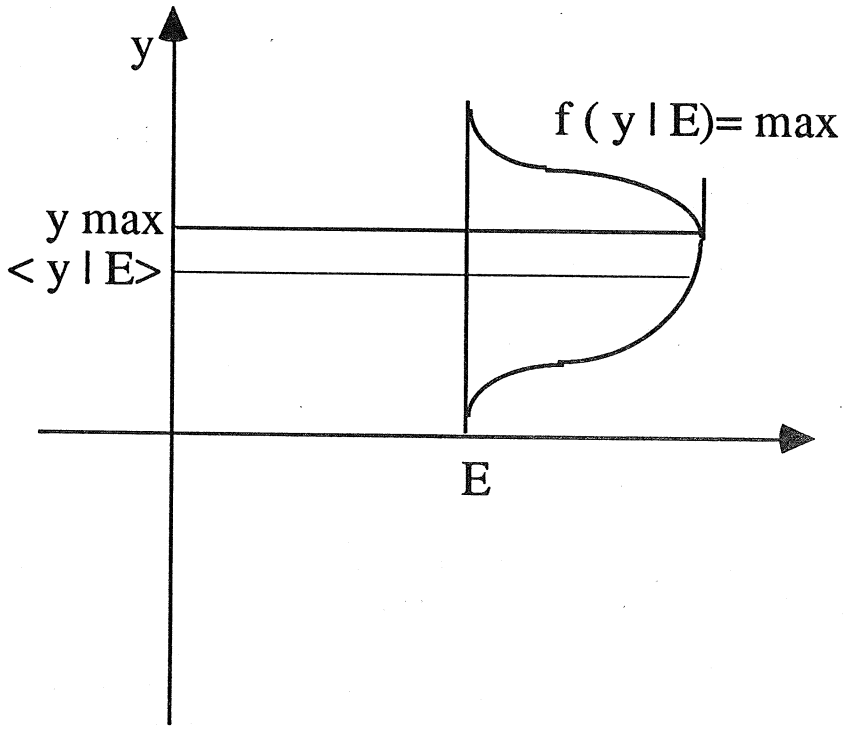

Figure 1.1 Maximum likelihood estimation and conditional averaging. The conditional average is the centroid of the conditional probability density function, whereas the maximum likelihood estimate of y is the location y_{max} at which the conditional probability density function reaches a maximum value.

$$\sigma^2_{y|E} = \int \left(\psi - \langle y \mid E \rangle\right)^2 f_{y|E}(\psi \mid E) d\psi . \tag{1.4}$$

If the conditional density is narrow, e.g. if

$$\sigma_{y|E} << \langle y \mid E \rangle \tag{1.5}$$

then both estimates are accurate. In general, either the maximum likelihood estimate or the conditional average is a useful form of estimation of y in terms of the available data E. They need not be the same, but in some situations they may be.

1.2 Stochastic estimation and turbulence structure.

The use of stochastic estimation to study turbulent flow is motivated by the desire to identify the "coherent structures" that are considered responsible for a significant part of the Reynolds stress and turbulent kinetic energy production, and by the need to specify a unique definition. Among the approaches generally used to search for and describe coherent structures in turbulent flows are:

- The study of individual realizations of the flow, in which one searches visually for patterns representing the "events".
- The study of spatial correlation functions:

$$R_{ij}(\mathbf{x},\mathbf{x}') = \left\langle u_i(\mathbf{x},t)u_j(\mathbf{x}',t)\right\rangle \tag{1.6a}$$

  or space-time correlation functions,

$$R_{ij}(\mathbf{x},\mathbf{x}',\tau) = \left\langle u_i(\mathbf{x},t)u_j(\mathbf{x}',t+\tau)\right\rangle \tag{1.6b}$$

  which are mathematically well-defined, but in which the features of coherent structures may be smoothed by the ensemble averaging operation.

- The study of conditional averages, which highlight the average velocity field associated with any chosen event. Conditional averages are precisely defined, and can be interpreted more easily than instantaneous realizations. The ensemble averaging process, of course, also smooths the data, but to a lesser extent than in correlations, since only a subset of the possible realizations is used in the conditional average.

Being well-defined mathematically, conditional averages can be a useful tool to understand and interpret correlations, thereby relating coherent structures to theory. They may, however, require large samples to obtain statistical convergence. Stochastic estimation is a way to estimate a conditional average given event vector $\mathbf{E}$ without actually performing conditional sampling.

The purpose of these lectures is to describe the application of stochastic estimation to the problem of educing structural information from empirical turbulence data obtained experimentally, or by numerical simulation. While maximum likelihood estimation is a useful method, it has proven difficult to use in turbulence. Consequently, the focus of these lectures will be on minimum mean square estimation, which includes conditional averages.

1.3 Linear and non-linear mean square estimation

In the context of turbulent structure identification the estimated variable is typically the velocity field $\mathbf{u}' = \mathbf{u}(\mathbf{x}',t')$ for some domain of positions and times, and the known variables

are associated with the occurrence of certain events at one or more points in the field. Their totality is referred to as the *event data vector,* **E**. We shall denote the estimate of $\mathbf{u}'$ by $\hat{\mathbf{u}}'$. It will be seen that *the best mean square estimate of* $\mathbf{u}'$ *given* **E**, *is the conditional average* $<\mathbf{u}'|\mathbf{E}>$. That is, of all possible estimates $\hat{\mathbf{u}}' = \mathbf{F}(\mathbf{E}), <|\mathbf{u}' - \mathbf{F}(\mathbf{E})|^2>$ is a minimum when $\mathbf{F} = <\mathbf{u}'|\mathbf{E}>$. In general, $<\mathbf{u}'|\mathbf{E}>$ is a non-linear function of **E**, but under the condition that the elements of $\mathbf{u}'$ and **E** are joint normally distributed, it is well known that $<\mathbf{u}'|\mathbf{E}>$ is a linear function of **E** (Papoulis 1984). Often, this property is applied approximately to non-normal random variables by postulating an estimate of $\mathbf{u}'$ in the form of a linear combination of the event data. Then one speaks of *linear mean square estimation.* This is a well known subject, thoroughly discussed in the literature of stochastic theory (Papoulis 1984; Deutsch 1965). The mean square error of the linear estimate must be greater than or equal to that of the conditional average.

Instead of estimating $\mathbf{u}'$ as some function of **E**, it is more straightforward conceptually to estimate the conditional average of $\mathbf{u}', <\mathbf{u}'|\mathbf{E}>$. The conditional average itself can always be interpreted as random variable since it is a function of **E**, and **E** is random. Then, it is natural to expand $<\mathbf{u}'|\mathbf{E}>$ in a Taylor series about **E**=**0**, and truncate at some level (Adrian 1977, Adrian 1979). When the series contains only first order terms, we refer to this as the *linear stochastic estimate (*LSE) to distinguish it from linear mean square estimation. In fact, it will be shown that the linear stochastic estimate of $<\mathbf{u}'|\mathbf{E}>$ and the linear mean square estimate of $\mathbf{u}'$ are numerically equal, so the principal difference is one of interpretation. For example, suppose that **E** that occurs at or near **x**. If $|\mathbf{x}-\mathbf{x}'|$ is large, $\mathbf{u}'$ is uncorrelated with **E**, and the mean square error of the linear estimate of $\mathbf{u}'$ must be large. On the other hand, under the same conditions, the error of the linear stochastic estimate of $<\mathbf{u}'|\mathbf{E}>$ may be small because $<\mathbf{u}'|\mathbf{E}>$ also vanishes as $|\mathbf{x}-\mathbf{x}'|$ becomes large.

The foregoing concepts can be illustrated simply by considering the estimation of a scalar random velocity $u' = u(x')$ given scalar event data E in the form of the value of $u(x)$ at x. We shall assume that $u(x')$ is a stationary, non-zero random process. Figure 1.2 shows a typical realization of $u(x')$ that passes through $u(x) = 1.5\sigma_1$., where σ_1 is the *rms* value. The conditional average $<u(x')|u(x)>$ is, of course, equal to u at $x = x'$, and therefore the error of the conditional average estimation vanishes at this point. As $|x-x'|$ increases, differences between $u(x')$ and $<u(x')|u(x)>$ appear, and the mean square error, $<[u(x') - <u(x')|u(x)>]^2>$ also increases. As $|x-x'|$ becomes large, $u(x')$ becomes statistically independent of $u(x)$ and consequently $<u(x')|u(x)>$ approaches $<u(x')>$, which is zero by assumption. Hence, the mean square estimation error starts at zero at $|x-x'|$=0, cf. Fig. 1.3, and increases to the level of one rms value of $u(x)$.as $/x'-x/$ approaches infinity.

Clearly, one must exercise caution not to overinterpret results obtained by conditional averaging. Even though the conditional average is the *best* mean square estimate, it may commit serious errors in regions that are weakly related to the event data. Interpretation

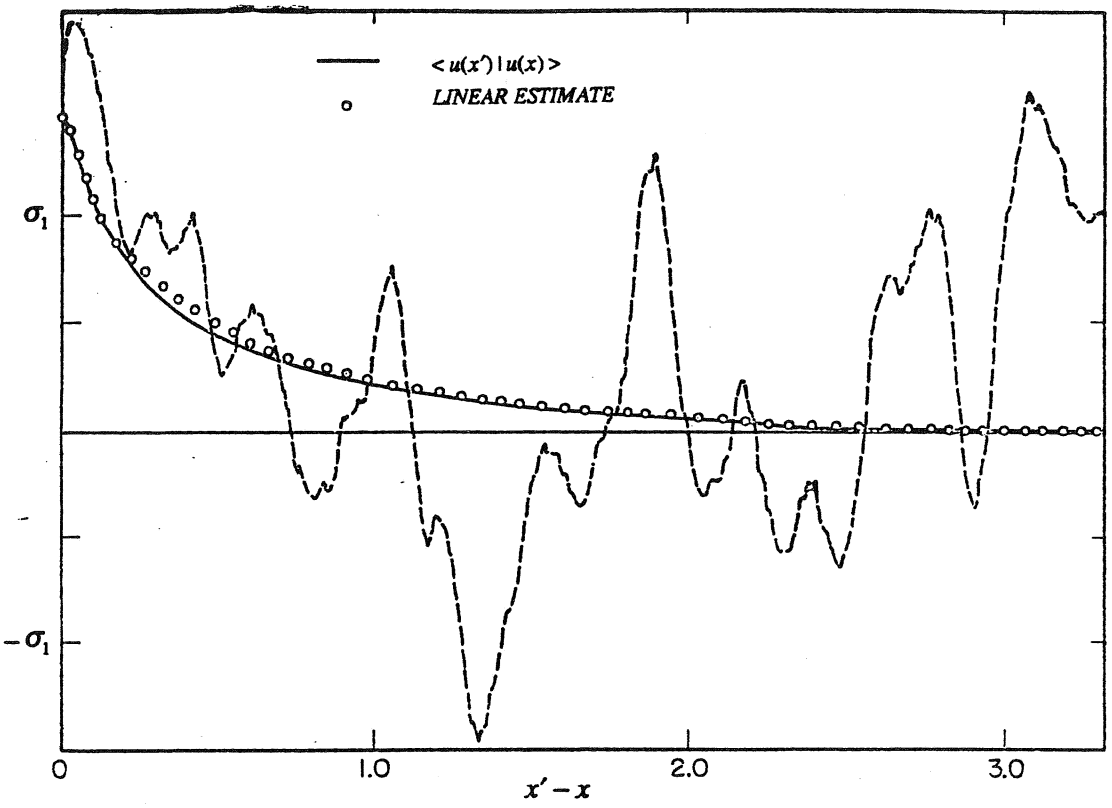

Figure 1.2 Conditional average of $u(x')$ given $u(x)= 1.5$ *rms,* and linear stochastic estimate compared to a random realization.

should always be made with the understanding that the conditional average may not look very much like any particular random realization. It always represents an average of many realizations. If each realization is very similar to every other realization, then the conditional average will itself look like a single realization. If there is significant variation between realizations, then the conditional average can only represent a mean structure. Even in this case, there is still no reason why one should not use conditional averages to describe structure, much as we find means, moments, and correlation functions to be useful, albeit imperfect descriptors of turbulent structure. Since stochastic estimates are approximations to the conditional averages, all of the foregoing observations pertain to them, as well.

Conditional averages are not perfect estimates of the random process itself, the linear stochastic estimate can only be worse. For the problem at hand, the linear estimate of $u(x')$ given $E=u(x)$ is

$$\hat{u}(x') = L(x,x')u(x) \tag{1.7}$$

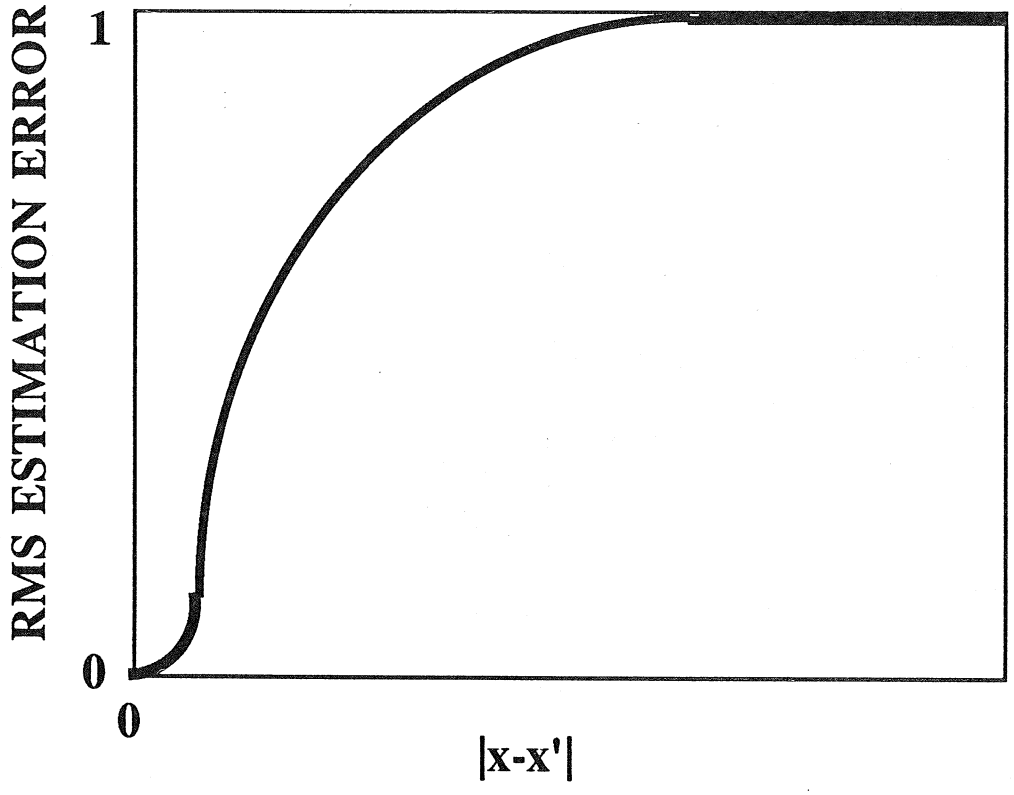

Figure 1.3 Mean square estimation error.

The mean square error is

$$e = \left\langle (u(x') - Lu(x))^2 \right\rangle, \tag{1.8}$$

and it is minimized by setting

$$\frac{\partial e}{\partial L} = 2\left\langle (u(x') - Lu(x))(-u(x)) \right\rangle = 0. \tag{1.9}$$

Eq (1.9) is satisfied if

$$L = \frac{R_{uu}(x,x')}{\left\langle u^2(x) \right\rangle}. \tag{1.10}$$

The linear stochastic estimate is also shown in Fig. 1.2. Note that it is very similar to the conditional average.

If we view $u(x')$ as a random variable, then $<u(x')\,|\,u(x)>$ is also a random variable by virtue of being a deterministic function of a random variable. Hence, we can also apply the linear stochastic estimation procedure to it. Let

$$\hat{u}(x') = \text{linear estimate of } \langle u(x')|u(x)\rangle = L(x,x')u(x). \tag{1.11}$$

As before, the mean square error is

$$e = \left\langle [\langle u(x')|u(x)\rangle - \hat{u}(x')]^2 \right\rangle, \tag{1.12}$$

and it is minimized by setting $\partial e/\partial L = 0$, which leads to

$$L\langle u^2(x)\rangle = \langle\langle u(x')\,|\,u(x)\rangle u(x)\rangle \tag{1.13a}$$

$$= \langle\langle u(x')u(x)\,|\,(u(x)\rangle\rangle \tag{1.13b}$$

$$= \langle u(x)u(x')\rangle \tag{1.13c}$$

$$= R_{uu}(x,x') \tag{1.13d}$$

Hence,

$$L = \frac{R_{uu}(x,x')}{\langle u^2(x)\rangle} \tag{1.14}$$

In (1.13b), use has been made of the fact that $u(x)$ is fixed by the conditional average so that it can be treated as a constant and taken inside the conditional brackets. Eq.(1.13c) is obtained by averaging over all $u(x)$ to reduce the conditional average to an unconditional average.

From (1.10) and (1.14) we see that *the linear estimate of the conditional average* of $u(x')$ is identical to the linear estimate of $u(x')$. Later, it will be shown that this is always true. If so, why distinguish between the two estimates? The reason is clear from Figure 1.2. While it may be that neither estimate is a good approximation to $u(x')$ itself, we see that *the linear estimate is an excellent approximation to conditional average*. It will be shown later that this is also true for all turbulent processes that have been investigated thus far. It is, therefore, always best to think of linear estimates as estimates of the conditional averages. A conditional average and its linear estimate may provide the same level of detail as a random realization if the event data is very detailed. Interestingly, the linear estimate provides a link between conditional averages and correlation functions. This linkage is a powerful result that

permits new interpretations of much of the body of common correlation and spectral analysis data.

The selection of event data has a profound influence on the conditional average and its linear estimate. How should E be specified? The correct approach is to design an event that corresponds to the physical question under investigation. Thus, if one selects E to be a large Reynolds stress event, $< \mathbf{u}' \mid \mathbf{E}(\mathbf{x}) >$ gives the average vector field around the site of the large Reynolds stress. The most famous event of this type is the quadrant analysis conditional average in which E is the event that $(u_1(\mathbf{x}), u_2(\mathbf{x}))$ lies in one of the four quadrants in the $u_1 - u_2$ plane:

$$Q1:(u_1>0,u_2>0);\ Q2:(u_1<0,u_2>0);\ Q3:(u_1<0,u_2<0);\ Q4:(u_1>0,u_2<0). \quad (1.15)$$

Points lying in the Q2 and Q4 quadrants contribute to positive values of the Reynolds shear stress $-<u_1u_2>$. A more specific condition is to specify the vector at x itself: $\mathbf{E}=\mathbf{u}(\mathbf{x})$. This not only states which quadrant $\mathbf{u}(\mathbf{x})$ lies in, but also the magnitude of its contribution to $-<u_1u_2>$.

To preview the sort of field that can be inferred from a linear stochastic estimate, consider the result in Fig. 1.4, obtained by estimating the vorticity field in the near wall region of low Reynolds number channel flow given a vector event u(x) that lies in the second quadrant of the u-v plane (Moin, Adrian and Kim 1987). The contours of constant magnitude of the fluctuating vorticity indicate a hairpin vortex with long legs trailing back along the wall. The legs are quasi-streamwise vortices, and their spacing is approximately one-hundred viscous wall units, corresponding to the well-known value for the spacing of low-speed streaks. It will suffice for now to note that this flow structure is very similar to the vortices observed in wall turbulence.

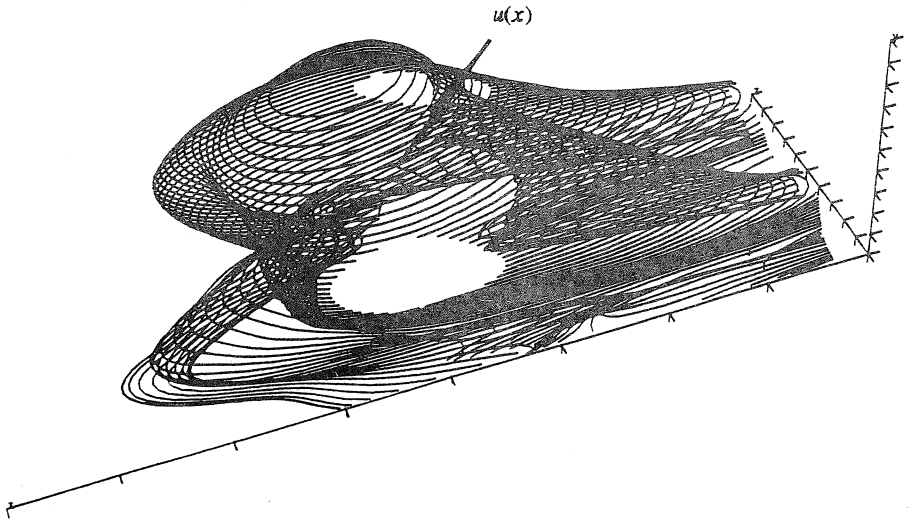

Figure 1.4 Stochastic estimate of the vorticity field of an eddy in low Reynolds number turbulent channel flow. The velocity at $y^+=49$ is specified to be a second quadrant event.

Events consisting of one or more vectors are natural in the probability density function equations of turbulence (c.f. Lundgren 1967, Monin 1967), as are events involving vorticity or deformation. *Table 1* lists various events that have been used in existing experimental studies. Note that events can become complicated very rapidly. For example, in Table 1, **d** is the deformation tensor, $d_{ij} = \partial u_i / \partial x_j$ which contains eight independent components in incompressible flow. In total, the event consisting of a three-dimensional vector **u** and all nine components of **d** spans an eleven dimensional space. One of the principal advantages of linear estimation of the conditional average is that it makes possible the use of relatively complicated events without sifting through very large spaces in search of realizations that satisfy the conditional event.

TABLE 1 Events used in analyses of turbulent fields by stochastic estimation.

E	Estimated Property	Reference
$\mathbf{u}(\mathbf{x},t)$	$\mathbf{u}(\mathbf{x},t')$	Adrian (1979), Hassan (1980), Moin, Adrian and Kim (1987)
$\mathbf{u}(\mathbf{x},t)$	$\mathbf{u}(\mathbf{x}',t)$	Adrian (1978, 1979), Hassan (1980), Tung & Adrian (1980), Tung (1982), Chang (1985), Chin (1987)
$\mathbf{u}(\mathbf{x},t)$	$u_i(\mathbf{x}',t)u_j(\mathbf{x}',t)$	Tung (1982), Elam (1987)
$\mathbf{u}(\mathbf{x},t)$	$p(\mathbf{x}',t)$	Chang (1985)
$p_{wall}(\mathbf{x},t)$	$u(\mathbf{x}',t)$	Willmarth & Wooldridge (1963)
$p(\mathbf{x}',t)$	$\mathbf{u}(\mathbf{x}',t)$	Nithianandan (1980)
$\mathbf{u}(\mathbf{x}_1,t),\mathbf{u}(\mathbf{x}_2,t)$	$\mathbf{u}(\mathbf{x}',t),\omega(\mathbf{x}',t)$	Adrian, Moin & Moser (1987)
$\mathbf{u}(\mathbf{x},t),\mathbf{d}(\mathbf{x},t)$	$\mathbf{u}(\mathbf{x}',t),\omega(\mathbf{x}',t)$	Adrian & Moin (1988), Ditter (1987)
$\tau_{wall}(x,t)$	$\mathbf{u}(\mathbf{x}',t),\omega(\mathbf{x}',t)$	Guezennec (1989)
$\phi(\mathbf{x},t)$	$\phi(\mathbf{x}',t)$	Pecseli (1987, 1991)

2. MEAN SQUARE ESTIMATION OF A RANDOM VARIABLE

2.1 Optimal mean square estimation

In this section we will establish results that were stated without proof in the Introduction, and generalize them to cover vector variables. Let $\hat{\mathbf{y}}$ be the estimate of a vector random variable y in terms of available data $\mathbf{E}=(E_1,...E_N)$. In general

$$\hat{\mathbf{y}} = \mathbf{F}(\mathbf{E}) \tag{2.1}$$

where **F** is a non-linear function of the data. The best mean square estimator is found by selecting **F** such that the error found by averaging over all values of the data

$$e = \left\langle | \mathbf{y} - \mathbf{F}(\mathbf{E}) |^2 \right\rangle \tag{2.2}$$

is a minimum. The ensemble average in (2.2) extends over y and **E**. The necessary condition for e to be a minimum is that its first variation with respect to **F** must vanish for arbitrary variations $\delta\mathbf{F}$:

$$\delta e = \left\langle 2[y_i - F_i(\mathbf{E})]\delta F_i \right\rangle = 0 \tag{2.3a}$$

Eq. (2.3a) can be solved by writing the unconditional average as the average of $<[y_i - F_i(\mathbf{E})]\delta F_i \mid \mathbf{E}>$ and then noting that $\delta F_i(\mathbf{E})$ can be taken outside of the conditional average since **E** is fixed inside the conditional average:

$$\delta e = 2\left\langle\left\langle [y_i - F_i]\delta F_i \mid \mathbf{E}\right\rangle\right\rangle \tag{2.3b}$$

$$= 2\left\langle\left\langle [y_i - F_i] \mid \mathbf{E}\right\rangle \delta F_i(\mathbf{E})\right\rangle \tag{2.3c}$$

The inner bracket in (2.3) averages over y keeping **E** fixed, and the outer bracket averages over **E**. Equation (2.3c) can be satisfied for any $\delta\mathbf{F}$ by setting $< y_i - F_i \mid \mathbf{E} >= 0$, or since $\langle \mathbf{F}(\mathbf{E}) \mid \mathbf{E} \rangle = \mathbf{F}(\mathbf{E})$,

$$\mathbf{F} = \langle \mathbf{y} \mid \mathbf{E} \rangle. \tag{2.4}$$

Thus, the best mean square estimate of y is its conditional average given all of the available data **E**, and in general this average is a non-linear function of **E**. It is clear that the mean square error will increase if not all of these data are used, or if the form of **F** is constrained.

The conditional average is related to the correlation functions by

$$\left\langle \langle y_i \mid \mathbf{E} \rangle E_j \right\rangle = \left\langle\left\langle y_i E_j \mid \mathbf{E}\right\rangle\right\rangle = \left\langle y_i E_j \right\rangle \tag{2.5}$$

Thus, *knowledge of* $< \mathbf{y} \mid \mathbf{E} >$ *and the probability density function of* $f(\mathbf{E})$ *is sufficient to determine* $< y_i E_j >$. The converse is not true: *Knowledge of the correlations* $< y_i E_j >$ *and* $f(\mathbf{E})$ *is not generally sufficient to determine* $< \mathbf{y} \mid \mathbf{E} >$.

2.2 Sub-optimal non-linear mean square estimation

Suppose the function $\mathbf{F}(\mathbf{E})$ is constrained to have some particular form

$$\mathbf{F}(\mathbf{E}) = \mathbf{F}_0(\mathbf{E}, \mathbf{p}) \tag{2.6}$$

where the vector $\mathbf{p}$ contains the parameters that appear in the form $\mathbf{F}_0$. For example, $\mathbf{F}_0$ could be a polynomial and the vector $\mathbf{p}$ could be a list of the coeffiecients of the polynomial. $\mathbf{F}_0$ may be non-linear, but since it is constrained to a form that may not coincide with $< \mathbf{y} \mid \mathbf{E} >$, the mean square estimation error must be greater than that of the optimal estimate given by the conditional average. The variational problem to minimize

$$e = \left\langle \mid \mathbf{y} - \mathbf{F}_0 \mid^2 \right\rangle \tag{2.7}$$

is

$$\frac{\partial e}{\partial p_j} = 0, \qquad j = 1,...J. \tag{2.8}$$

where J is the number of adjustable parameters in $\mathbf{F}_0$. The reader will recognize the problem of finding a non-linear, sub-optimal estimate in this way as the Rayleigh-Ritz method from variational calculus.

2.3 Linear mean square estimation

Suppose that the form of $\mathbf{F}_0$ is restricted further to be linear in the event data:

$$\hat{y}_i = F_{oi}(\mathbf{E}) = A_i + L_{ij} E_j, \qquad i = 1,...,I \tag{2.9}$$

(The summation convention applies to repeated Latin subscripts.) One expects this restriction to further increase the estimation error. The necessary conditions for minimum mean square error are

$$\frac{\partial e}{\partial A_k} = 0, \qquad k = 1,..,I \tag{2.10a}$$

$$\frac{\partial e}{\partial L_{il}} = 0, \qquad i = 1,...,I, \quad l = 1,...,N \tag{2.10b}$$

Substituting (2.9) into (2.10) and applying these conditions gives the following set of equations:

$$A_i + \langle E_j \rangle L_{ij} = \langle y_i \rangle, \quad i = 1,..,I \quad and \quad l = 1,..,N \tag{2.11a}$$

$$A_i \langle E_l \rangle + \langle E_j E_l \rangle L_{ij} = \langle y_i E_l \rangle, \quad i = 1,..,I, \quad j,l = 1,..,N \tag{2.11b}$$

These equations are in terms of variables y and E that may have non-zero mean values. They become decoupled if E and y are decomposed into mean and fluctuating parts. Then, equation (2.11b) reduces to the following system of linear algebraic equations for L_{ij}

$$\langle (E_j - \langle E_j \rangle)(E_l - \langle E_l \rangle) \rangle L_{ij} = \langle (y_i - \langle y_i \rangle)(E_l - \langle E_l \rangle) \rangle \tag{2.12}$$

whence equation (2.11a) can be solved for A_i.

From (2.12) it is clear that the mean values of the event data have no influence on the coefficients L_{ij}. If we agree to use only zero mean event data, the equations for L_{ij} simplify to

$$\langle E_j E_l \rangle L_{ij} = \langle y_i E_l \rangle, \qquad i = 1,...I \quad and\, j,l = 1,...N. \tag{2.13}$$

These equations are known as the *Yule-Walker* equations (Papoulis 1984). They give the estimation coefficients in terms of the correlation functions $\langle E_j E_l \rangle$ between each of the data, and the correlation function $\langle y_i E_l \rangle$ between the data and the estimated variable. Hereafter we shall assume the $\langle E_l \rangle = 0$.

The *Orthogonality Principle* states that the condition for minimizing the mean square error of the linear estimate is that the errors must be *statistically orthogonal* to the data (i.e. they must be statistically uncorrelated). With $\langle E_l \rangle = 0$ a simple rearrangement of (2.13) shows that the error y_i-$L_{ij}E_j$ is indeed orthogonal to E_l:

$$\langle (y_i - L_{ij} E_j) E_l \rangle = 0, \quad i = 1,...I, \quad j,l = 1,..,N. \tag{2.14}$$

The mean square error of the linear estimate is found from

$$e = \langle (y_i - L_{ij}E_j)(y_i - L_{ik}E_k) \rangle \tag{2.15a}$$

$$= \langle (y_i - L_{ij}E_j) y_i \rangle = \langle y_i y_i \rangle - \langle \hat{y}_i\, y_i \rangle. \tag{2.15b}$$

Suppose that **y** is correlated with the data, but the data are uncorrelated with each other. Then

$$\langle E_j E_l \rangle = \langle E_j{}^2 \rangle \delta_{jl}$$

and the data correlation matrix $< E_j E_l >$ becomes diagonal, leading immediately to the simple solution

$$L_{il} = \langle y_i E_l \rangle / \langle E_l{}^2 \rangle \tag{2.16}$$

If **y** is statistically independent of every datum, $< y_i E_j >= 0$, then (2.13) becomes a homogeneous set of equations for L_{ij}, and if

$$\det \langle E_j E_l \rangle \neq 0, \tag{2.17}$$

the only solution for L_{ij} is the trivial solution. Then $\hat{\mathbf{y}} =< \mathbf{y} >$, which shows that a non-trivial linear estimate cannot be obtained unless the given data are correlated with **y**.

It is helpful to consider a simple example in which the variable to be estimated is $y = u' = u(x')$ and the data consist of the value of u at x, as in Fig. 1.2. Then

$$\hat{u}' = L(x, x')u(x) \tag{2.18}$$

and the orthogonality principle requires

$$\langle (u' - Lu(x))\, u(x) \rangle = 0 \tag{2.19}$$

or

$$L = \frac{R_{uu}(x, x')}{R_{uu}(x, x)} \tag{2.20}$$

where

$$R_{uu}(x, x') = \langle u(x)u(x') \rangle. \tag{2.21}$$

Hence

$$\hat{u}(x') = \frac{R_{uu}(x,x')}{R_{uu}(x,x)}\, u(x). \tag{2.22}$$

The normalized mean error is

$$\frac{e}{\langle u'^2 \rangle} = 1 - \frac{\langle u' \hat{u}' \rangle}{\langle u'^2 \rangle} = 1 - \frac{R_{uu}{}^2(x,x')}{R_{uu}(x',x')R_{uu}(x,x)}. \tag{2.23}$$

Suppose u(x) is statistically homogeneous in x with Taylor microscale λ_τ defined by

$$\frac{R_{uu}(x-x')}{R_{uu}(x,x)} \cong 1 - \frac{|x-x'|^2}{\lambda_\tau{}^2}. \tag{2.24}$$

Then the error approaches zero as

$$\frac{e}{\langle u^2 \rangle} \sim \frac{2|x-x'|^2}{\lambda_\tau{}^2} \tag{2.25}$$

Thus, the linear estimate of a random variable *u(x)* is accurate only for separations between the estimated variable and the data which are smaller than the Taylor microscale.

3. MEAN SQUARE ESTIMATION OF CONDITIONAL AVERAGES

3.1 Governing Equations

The concept of using mean square estimation to approximate a *conditional average* was introduced in Section 1. In this section, this idea will be explored in more detail, and developed for general event vectors.

Suppose that $\mathrm{y}' = \mathrm{y}(\mathrm{x}',t')$ is any quantity of interest. The conditional average of y' given $\mathbf{E}$ must be a function of the variables $(\mathbf{E},\mathrm{x}',t')$ plus, implicitly, any space-time locations that are involved in specifying the event data. $<\mathrm{y}'\,|\,\mathbf{E}>$ is a deterministic function of these variables, and since it is an average, it tends to be a smoother function of (x',t') than the underlying random field. One also expects that $<\mathrm{y}'\,|\,\mathbf{E}>$ would depend smoothly upon the data, e.g., continuous changes in $\mathbf{E}$ produce continuous changes in the conditional average. (For arguments concerning when this may not always be the case, c.f. Novikov 1993.) Assuming that $<\mathrm{y}'\,|\,\mathbf{E}>$ is a continuous function of $\mathbf{E}$, one can expand it in a Taylor series, the natural points of expansion being the most probable value of $\mathbf{E}$, or, more conveniently, the mean value of $\mathbf{E}$. If we assume that the event vector represents fluctuations with respect to the mean, then Taylor series expansion about $\mathbf{E}=\mathbf{0}$ corresponds to analysis of *weak* fluctuations:

$$\langle y_i' \mid \mathbf{E} \rangle = A_{ij}E_j + B_{ijk}E_jE_k + C_{ijkl}E_jE_kE_l + 0(E^4) \tag{3.1}$$

The coefficients A, B, C,... are undetermined functions of $(\mathbf{x},'t')$and the locations of the event data. Other forms of expansion could be used, but the foregoing is natural because it leads to results that involve standard central moments of **E**.

Minimizing the mean square error leads to the following set of equations for the coefficients

$$\langle [\langle y_i' \mid \mathbf{E} \rangle - A_{ij}E_j - B_{ijk}E_jE_k - ...]E_l \rangle = 0 \tag{3.2a}$$

$$\langle [\langle y'_i \mid \mathbf{E} \rangle - A_{ij}E_j - B_{ijk}E_jE_k - ...]E_lE_m \rangle = 0, \tag{3.2b}$$

and so on. These equations may or may not be coupled, depending on the statistical correlations $< E_jE_l >, < E_jE_kE_l >$, etc. Also, because of the additional terms in the power series, the coefficient A_{ij} of the linear term may not be equal to the linear estimation coefficient L_{ij}.

If the estimate is restricted to a *linear form*, the governing equation for the linear estimation coefficients are

$$\langle E_jE_l \rangle A_{ij} = \langle y_i'E_l \rangle, \quad i = 1,...I \ \ and \ \ j,l = 1,...,N \tag{3.3}$$

These are identical to the Yule-Walker equations for estimation of **y** in terms of **E**, so we see that A_{ij}=L_{ij}. if the estimate is linear.

Although there is no numerical difference between these estimates, their interpretations are quite different, as discussed previously. When estimating **y** in terms of **E**, one might hope that the estimate would be a good approximation to $\mathbf{y}(\mathbf{x}',t)$. But, of course, as $\mathbf{y}(\mathbf{x}',t)$ is moved away from the data locations, so that correlation between **E** and **y** is lost, the accuracy of approximation decreases. Thus, when estimating $< \mathbf{y}' \mid \mathbf{E} >$ directly, one realizes that $< \mathbf{y}' \mid \mathbf{E} >$ itself is an estimate of $\mathbf{y}'$ that has limited accuracy. Deviations of $< \mathbf{y}' \mid \mathbf{E} >$ from $\mathbf{y}'$ are accepted as part of the information loss that occurs when one characterizes random fields by statistical quantities.

The more interesting aspect of stochastic estimation is the fact that conditional data are found from the unconditional moments. Put another way, one can find conditionally averaged behavior, without performing conditional sampling. The practical implications of this property will be discussed later.

3.2 Joint normal random processes.

The accuracy of stochastic estimation of conditional averages is, of course, an important issue. In this regard, the class of joint normally distributed random variables

provides an important reference case, because *if the random variables* $\mathbf{y}'$ *and* $\mathbf{E} = (E_1,...E_N)$ *are joint normally distributed, then the conditional average* $<\mathbf{y}'\,|\,\mathbf{E}>$ *is given exactly by the linear estimate, as specified by the leading term in (3.1) and (3.3).* Since joint normal probability distributions are determined completely by the first and second moments of the random variables, it should not be surprising that the conditional average can be found through equations like (3.3) which involve only $< E_l E_m >$ and $< y_i' E_l >$.

The proof of the foregoing result is instructive. Suppose without loss of generality that $< y_i' >=< \mathbf{E} >= 0$. If the variables E_j are joint normally distributed, then the sum $L_{ij}E_j$ is also a normal random variable (Papoulis 1984). Likewise, if y_i' is joint normally distributed with respect to E_j, then the difference, $y_i' - L_{ij}E_j$ is also a normal random variable. For linear estimation, the coefficients L_{ij} are chosen to satisfy

$$\langle [y_i' - L_{ij}E_j]E_k \rangle = 0, \quad i = 1,...I \;\; and \;\; j,k = 1,...N \tag{3.4}$$

which states that $y_i' - B_{ij}E_j$ is uncorrelated with each E_k. But, joint normal random variables that are uncorrelated are also statistically independent (Papoulis 1984). Hence, if $y_i' - L_{ij}E_j$ is statistically independent of $\mathbf{E}$, then

$$\left\langle y_i' - L_{ij}E_j \,|\, \mathbf{E} \right\rangle = \left\langle y_i' - L_{ij}E_j \right\rangle \tag{3.5a}$$

$$= \langle y_i' \rangle - L_{ij} \langle E_j \rangle \tag{3.5b}$$

$$= 0 \tag{3.5c}$$

because $=< y_i' >=< E_j >= 0$ by assumption. But, also

$$\left\langle y_i' - L_{ij}E_j \,|\, \mathbf{E} \right\rangle = \langle y_i' \,|\, \mathbf{E} \rangle - L_{ij}E_j \tag{3.6}$$

so, upon combining (3.5c) and (3.6) we have exactly

$$\langle y_i' \,|\, \mathbf{E} \rangle = L_{ij}E_j . \tag{3.7}$$

It should be noted that the key property of joint normal processes that is needed to make the foregoing proof is the fact that joint normality implies that uncorrelated random variables are statistically independent.

3.3 Non-normal random processes

Any other process for which uncorrelatedness implies independence would also have a conditional average given exactly by the linear stochastic estimate. Joint normality implies zero error for LSE, but this does not mean that LSE must be inaccurate if the processes are not joint normal. To illustrate, a situation in which the conditional average of a non-normal random process can be exactly linear, consider Figure 3.1. Fig. 3.1(a) shows the elliptical contours that are characteristic of a joint normal *pdf* relationship between y' and E. The conditional average, being the centroid of the *pdf* at fixed E, is a linear function of E (see also Figure 1.1). Next, consider the decidedly non-Gaussian contours of the non-normal *pdf* in Figure 3.1(b). It has been drawn so that its centroidal masses are also located on a linear function of E, with the consequence that the linear form of the conditional average would also be correct for this distribution.

The accuracy of LSE has been tested in various turbulent flows by measuring the conditional average and the correlation functions needed to estimate them. Figure 3.2 compares the linear estimate to the conditional average of the time-delayed streamwise velocity $< u,(x,t+\tau) \mid u,(x,t) >$ in grid turbulence for several different values the velocity at zero time delay. These curves correspond to Figure 1.2. Although the agreement is good, one might argue that grid turbulence is an easy test because it is weak.

Figure 3.3 compares the conditional average of the time-delayed streamwise velocity on the centerline of an axisymmetric jet to its LSE. In this flow, the turbulence intensity is much higher than in grid turbulence, and the turbulence statistics are decidedly non-normal. The curves are normalized by the data $E = u_1(x,t)$ to make the linearity of the relationship apparent. Agreement is generally good, although the data at $x_1/D = 3$ shows some non-linear dependence upon the event data.

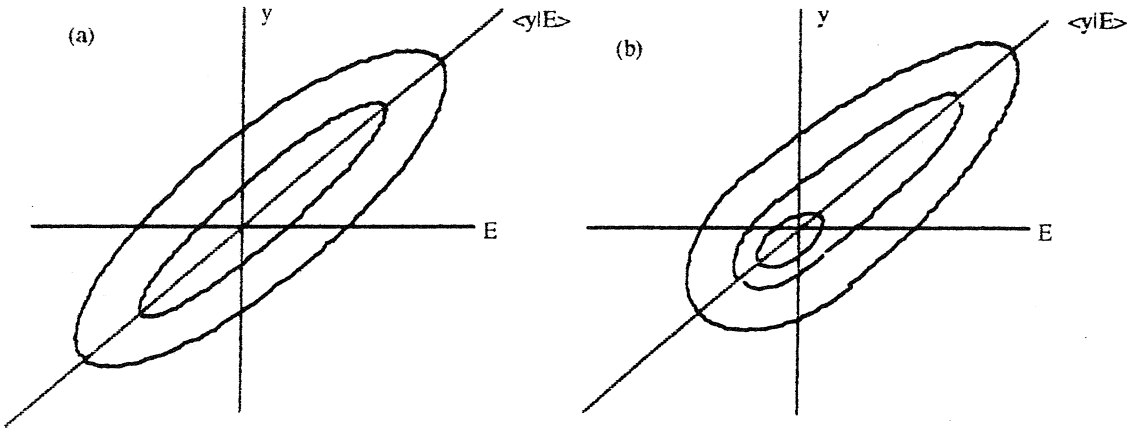

Figure 3.1 (a) Conditional average of joint normal variables (y,E) is linear; (b) a linear conditional average is also possible for non-normal random variables.

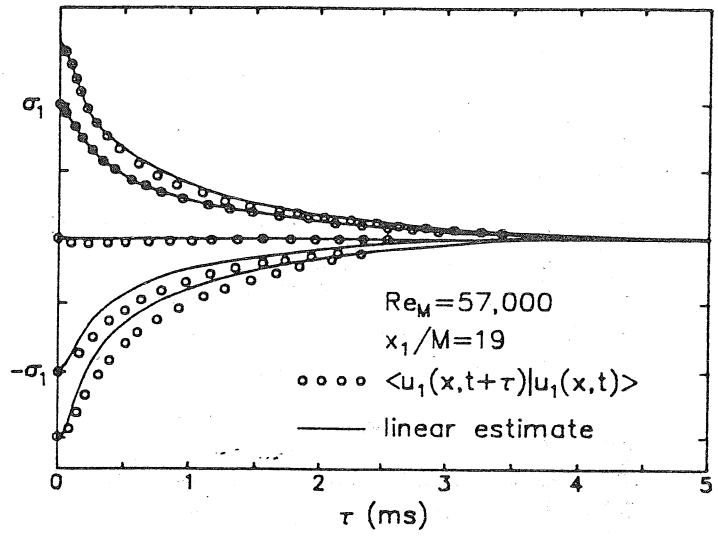

Figure 3.2 The conditionally averaged, time-delayed conditional velocity and linear estimate in grid turbulence for $u_1(x,t)/\sigma_1 = -1.5, -1.0, 0, 1.0,$ *and* 1.5. *[Adrian et al. 1989].*

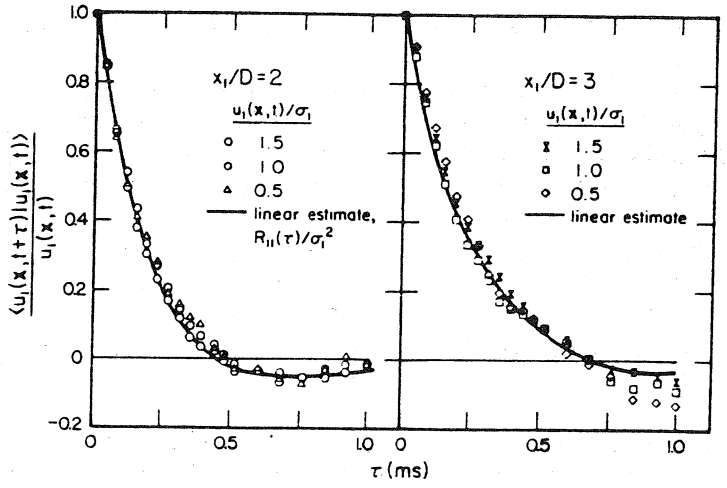

Figure 3.3 A comparison of conditionally averaged streamwise velocity to its linear estimate on the centerline of an axisymmetric shear layer. *[from Adrian et al. 1989].*

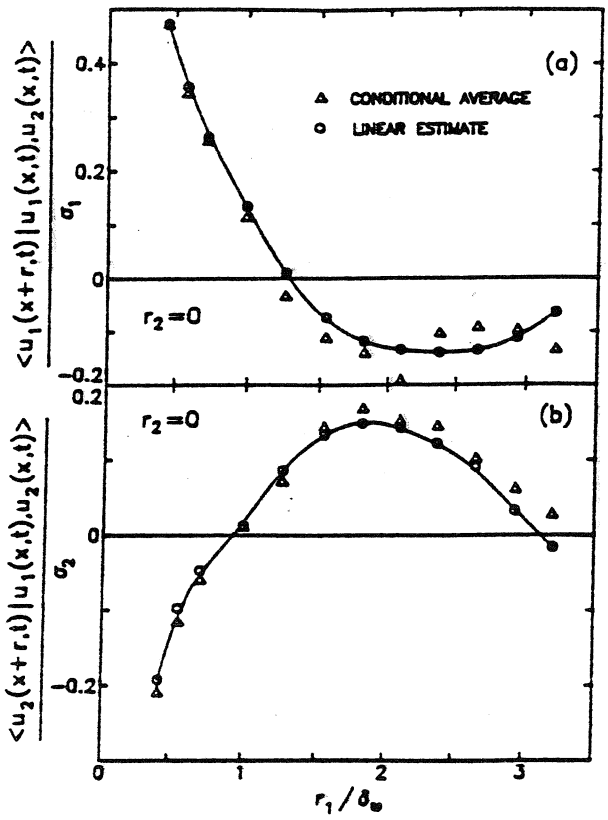

Figure 3.4 Conditional average and linear estimates on the centerline of a plane turbulent shear layer. (a) streamwise velocity; b) cross-stream velocity *[from Adrian et al. 1989].*

Figures 3.4 and 3.5 each contain estimates of velocities that are separated from the event data in space, instead of time. Figure 3.4 contains measurements from a two-stream mixing layer in which the conditional event consists of two events: the streamwise velocity and cross-stream velocity on the shear layer centerline. The turbulence intensity is also large.

Figure 3.5 shows results for the streamwise velocity in pipe flow. The measurements in this experiment suffered from insufficient time averaging, resulting in some sampling error noise in the correlation functions and in the conditional averages. This noise is manifested in the small amplitude irregularities of the curves in Fig. 3.5. Interestingly, the sampling noise appears to be similar in both quantities.

To assess the significance of non-linear terms in the estimates, Figure 3.5 compares the linear estimate to an estimate containing quadratic terms. There is relatively little difference in this particular flow, a pipe flow, but as pointed out by Guezennec (1989), the non-linear terms are necessary if one hopes to see any difference in the conditional patterns due to a change in the sign of the event data. Thus for example, to within the limits of linear estimation there is no difference between the conditional average given a Q2 event vector and and identical but opposite Q4 event vector, aside from a change in the sign of the conditional field. Addition of quadratic or higher order terms alters this situation, but the results of

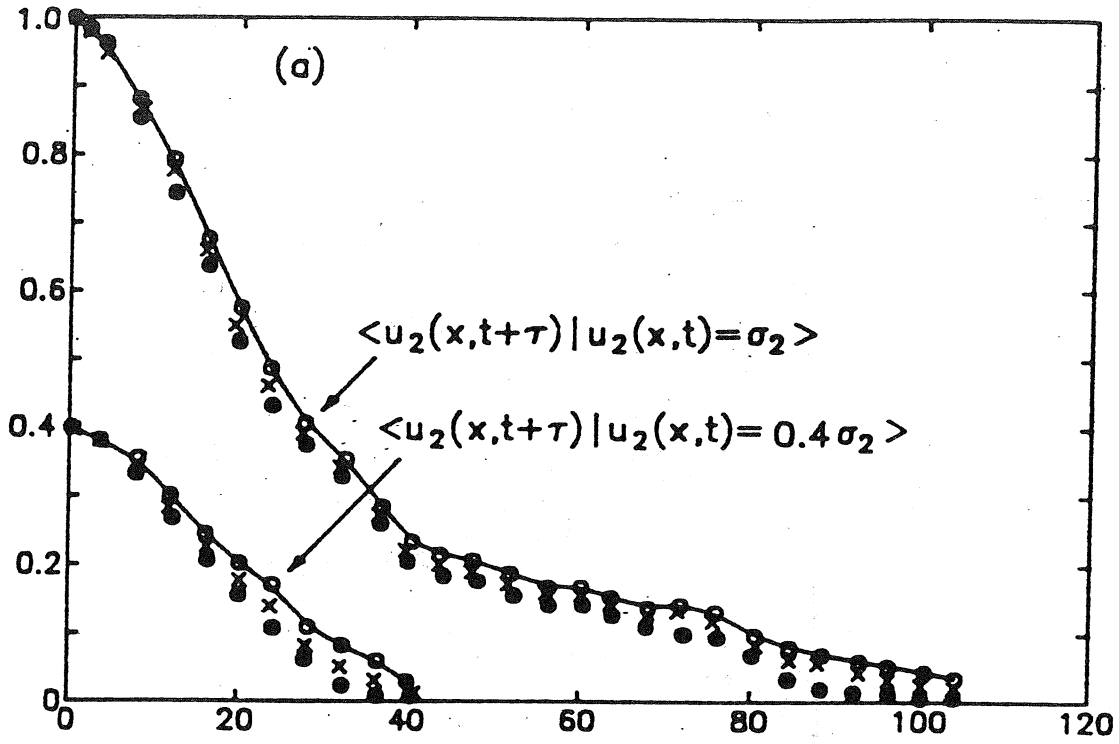

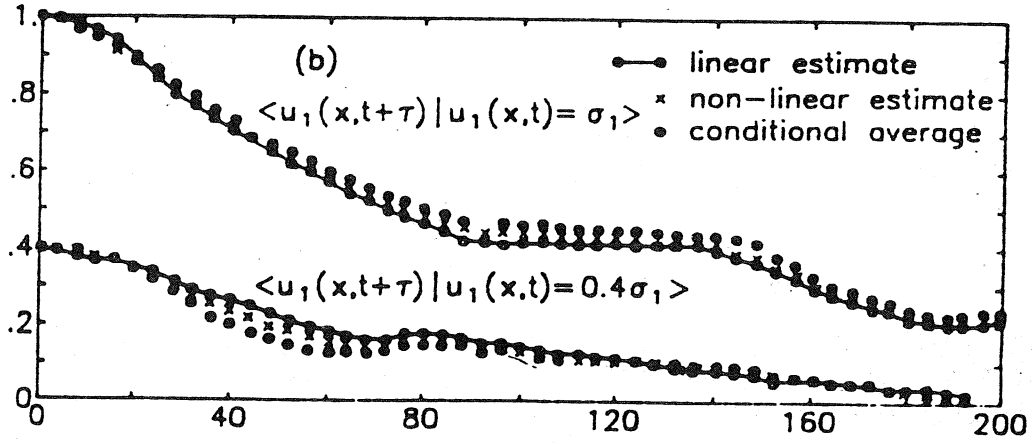

Figure 3.5 Conditional averages and linear estimates in the outer region of turbulent pipe flow at 50,000 Reynolds number. *[From Hassan 1980, c.f. also Adrian et al. 1989].*

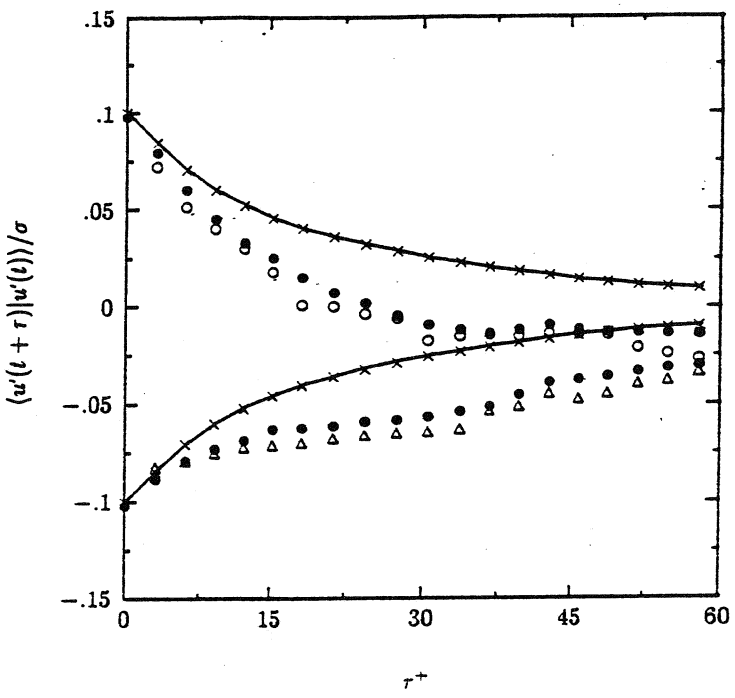

Figure 3.6 Improved approximation of conditional averages given low amplitude events. $o, < u(t+\tau) \mid u(t) = 0.1\sigma_1 >$; $\Delta, < u(t+\tau) \mid u(t) = -0.1\sigma_1 >$; $\times$, *LSE*; −, quadratic MSE; • Laurent series MSE. *[From Brereton 1992].*

Guezennec (1989) do not produce noticeable change. It may be that the principal difference associated with a change in the sign of the event vector occurs when the conditional average of the fluctuating velocity is added to the mean flow.

In general, the experimental evidence supports the idea that linear estimation of conditional averages is a reasonably accurate procedure, even when the random processes involved are non-normal. Some steps have been made to improve on LSE. For example, Brereton (1992) has observed that the expansion may be postulated to contain a term like $S_{ij}E_j^{-1}$ so that the expansion can emphasize the importance of low amplitude events. Evidence that such a Laurent-like series offers improved approximations was obtained in a boundary layer, Figure 3.6.

3.4 Summary

Conditional averages of turbulent quantities can be approximated rather well by the linear and non-linear mean square estimation. In general, linear estimation is adequate, but non-linear estimation offers more improvement as well as some conceptual advantages. The estimation results are expressed in terms of correlation functions which must be known from some other mean such as experiment. The advantages of stochastic estimation relative to conditional averaging are:

- Complicated events can be used with the estimation procedure.
- Stochastic estimates are more stable than conditional averages because they use all of the data in forming the correlation functions.
- Once the stochastic estimates are formed, the numerical values of the conditional events may be changed easily to fully explore the event space.

4. CONDITIONAL EDDIES

4.1 Definition

It is widely recognized that the use of a conditional average $< \mathbf{u}' \mid \mathbf{E} >$ to characterize coherent motions runs the risk of obtaining results that are more representative of the conditional event than of the coherent structure. This is a legitimate concern, and for this reason it is, in the author's opinion, a mistake to interpret a conditional average as always being truly representative of instantaneous structure. Rather, one should only interpret it as an average field associated with the occurrence of the event - no more and no less. In certain instances the conditional average may correspond very closely to the instantaneous structures. This occurs, for example if the field contains many structures that all look similar. But, if the field consists of many different types of structures that each satisfy the conditional event, then the conditional average will be an average over all of the different types. Hence, in general, it is best to treat conditional averages as statistical quantities that characterize certain average features of a flow field, just as the mean, rms, pdf, correlation and power spectrum each characterize different aspects. Being conditional does not guarantee, by itself, that the average will give a very realistic picture of the coherent structure, and indeed, it has been shown in Section 1 that substantial differences do occur.

The fidelity with which a conditional average can represent turbulent structure depends strongly upon the information contained in the event. Given sufficiently complex data, it is possible to perfectly reconstruct the entire turbulent velocity field. But, this would not be a coherent structure. Given too little data, it is possible to get a field that bears little resemblance to a coherent realization. Between these limits, there may or may not be an event or set of events that faithfully reproduces all aspects of a coherent realization. Thus, in general, the conditional average is only an imperfect representative of coherent structure, and it is best to avoid implications to the contrary by carefully distinguishing between coherent structures and conditional fields $< \mathbf{u}(\mathbf{x}',t') \mid \mathbf{E} >$. To do so, we shall refer to the latter as *conditional eddies* (Adrian 1979). The intention behind introducing this term is to define the

conditional eddies as mathematical entities, and thereby separate the issue of existence from the issue of how well they correspond to a coherent structure. For example, while one might doubt the existence of coherent structure in a highly chaotic, high Reynolds number flow, there can be no argument concerning the existence of conditional eddies; they must exist because it must be possible to define a conditional average of $\mathbf{u}(\mathbf{x}',t')$.

The conditional eddy field depends upon the type of event **E**, and the proper definition of **E** is clearly critical to the formation of a useful conditional eddy concept. In fact, it is fair to say that many of the research questions concerning conditional eddies revolve around the definition of **E**. Fortunately, the equations of fluid mechanics suggest natural forms.

Consider, for example, the one-point probability density function of the turbulent velocity at **x**:

$$f_1(\mathbf{v},\mathbf{x},t) = \text{Prob}\{\mathbf{v} \le \mathbf{u}(\mathbf{x},t) < \mathbf{v} + \mathbf{dv}\}d\mathbf{v}. \tag{4.1}$$

The Lundgren-Monin equation (Lundgren 1967, Monin 1967) for this probability density can be wriitten in the form

$$\frac{\partial f_1}{\partial t} = \frac{\partial}{\partial v_i}\left\{\left\langle \frac{\partial u_i}{\partial t}|\mathbf{v}\right\rangle f_1(\mathbf{v},\mathbf{x},t)\right\} \tag{4.2}$$

where the conditional time derivative is given by

$$\left\langle \frac{\partial u_i}{\partial t}\middle|\mathbf{v}\right\rangle = \lim_{\mathbf{x}'\to\mathbf{x}}\left\{-v_j\frac{\partial}{\partial x_j'}\langle u_i'|\mathbf{v}\rangle - \frac{1}{\rho}\frac{\partial}{\partial x_i'}\langle p'|\mathbf{v}\rangle + \nu\frac{\partial^2}{\partial x_l'^2}\langle u_i'|\mathbf{v}\rangle\right\} \tag{4.3}$$

It is well known that equation (4.2) contains pressure and viscous terms that are unclosed because they depend upon the two-point *pdf* of the turbulent velocities. As shown by equation (4.3) this dependence occurs fundamentally because the conditional stress terms on the right hand side of (4.3) each require a conditionally averaged field to be evaluated, either $\langle p'|\mathbf{v}\rangle$ or $\langle \mathbf{u}'|\mathbf{v}\rangle$. These terms correspond to the one-point conditional eddy. Thus, the closure problem for the one-point *pdf* equation is essentially one of modeling the conditional eddy given the velocity at one point. The problem is complicated somewhat by the fact that the conditional pressure is given by the solution of the Poisson equation

$$\nabla'^2\langle p'|\mathbf{v}\rangle = -\rho\frac{\partial^2}{\partial x_i'\partial x_j'}\langle u_i'u_j'|\mathbf{v}\rangle \tag{4.4}$$

which involves the conditional Reynolds stress as well as the conditional eddy.

More generally the N-point *pdf* equation depends upon the N+1-point *pdf*. It has also been shown (Adrian 1977) that the unclosed terms, aside from the pressure term, always have the form of a conditional average given the turbulent velocities at N points, e.g.,

$$< \mathbf{u}(\mathbf{x}',t) \mid \mathbf{u}(\mathbf{x},t) = \mathbf{v}_1,...,\mathbf{u}(\mathbf{x}_N,t) = \mathbf{v}_N >. \tag{4.5}$$

Thus, at every level in the hierarchy of *pdf* equations, a conditional eddy appears which is increasingly more detailed as the level of the hierarchy increases. The locations $\{ \mathbf{x}_1,\mathbf{x}_2,...,\mathbf{x}_N \}$ are variables in the *pdf* equation, and in particular, one point may be made to coincide with another so that an N-point conditional eddy can be reduced to an N-1 point conditional eddy. A *one-point* conditional eddy is of the form $< \mathbf{u}(\mathbf{x}',t) \mid \mathbf{u}(\mathbf{x},t) >$ where the data event $\mathbf{u}(\mathbf{x}_1,t)$ is located at $\mathbf{x}_1 = \mathbf{x}$.

A second type of conditional eddy is defined by using the local vorticity, $\omega(\mathbf{x})$ (Novikov 1967) or more generally the local deformation tensor

$$d_{ij} = \frac{\partial u}{\partial xj} \tag{4.6}$$

as events which specify the local rotation and deformation of the flow (Adrian and Moin 1987). The local velocity $\mathbf{u}(\mathbf{x},t)$ plus the local deformation tensor are sufficient to specify the state of motion at $\mathbf{x}$ in term of translation, rotation, and strain rate.

4.2 Properties of conditional eddies

Consider a general conditional eddy $< \mathbf{u}' \mid \mathbf{E} >$. The following reduction properties are statistical in nature

$$\langle\langle \mathbf{u}' \mid \mathbf{E} \rangle\rangle = \langle \mathbf{u}' \rangle \tag{4.7a}$$

$$\langle\langle \mathbf{u}' \mid \mathbf{E} \rangle \mid \mathbf{E}_s \rangle = \langle \mathbf{u}' \mid \mathbf{E}_s \rangle \tag{4.7b}$$

where $\mathbf{E}_s$ is a subset of $\mathbf{E}$. They describe the reduction of a conditional eddy to another conditional eddy with simpler event. If the elements of $\mathbf{E}$ are located at $\mathbf{x}$, then

$$\lim_{|\mathbf{x}'-\mathbf{x}| \to \infty} \langle \mathbf{u}' \mid \mathbf{E} \rangle = \langle \mathbf{u}' \rangle \tag{4.8}$$

because $\mathbf{u}'$ becomes statistically independent of $\mathbf{E}(\mathbf{x})$ as $|\mathbf{x}'-\mathbf{x}|$ becomes large. More generally a relation like (4.8) holds if $\mathbf{E}$ consists of multipoint events that are clustered around $\mathbf{x}$ within a sphere of finite radius.

Suppose $\mathbf{E}$ contains an event like $\mathbf{u}(\mathbf{x})=\mathbf{v}$. Then

$$\lim_{\mathbf{x}' \to \mathbf{x}} \langle \mathbf{u}'(\mathbf{x}) \mid \mathbf{E} \rangle = \mathbf{u}(\mathbf{x}) = \mathbf{v} \tag{4.9}$$

If $\mathbf{E}$ contains multipoint events $\mathbf{E} = \{\mathbf{u}(\mathbf{x}_\alpha) = \mathbf{v}_\alpha,\ \alpha = 1,...,N\}$ then a relation similar to (4.9) holds for every point. Thus, the conditional eddy is like an interpolating function that is pinned to the data points.

Since $\mathbf{E}$ is independent of $\mathbf{x}'$, the operations of conditional averaging and differentiation with respect to $\mathbf{x}'$ commute. Then

$$\left\langle d_{ij}' \mid \mathbf{E} \right\rangle = \frac{\partial}{\partial x_j'} \left\langle u_i' \mid \mathbf{E} \right\rangle \tag{4.10}$$

i.e., the conditional average of the deformation field is the deformation of the conditional eddy velocity field. Clearly, a similar statement pertains to the vorticity, and if the flow is incompressible, the conditional eddy field is solenoidal:

$$\frac{\partial}{\partial x_i'} \left\langle u_i' \mid \mathbf{E} \right\rangle = 0. \tag{4.11}$$

Given a conditional eddy, the unconditional average of the product of $\mathbf{u}'$ with any function $\mathbf{Q}(\mathbf{E})$ can be found by averaging:

$$\left\langle \mathbf{Q}(\mathbf{E}) \left\langle \mathbf{u}' \mid \mathbf{E} \right\rangle \right\rangle = \left\langle \left\langle \mathbf{Q}\mathbf{u}' \mid \mathbf{E} \right\rangle \right\rangle \tag{4.12a}$$

$$= \left\langle \mathbf{Q}(\mathbf{E})\mathbf{u}' \right\rangle \tag{4.12b}$$

The averaging requires, in principle, the *pdf* $f_{\mathbf{E}}$. The function Q can contain any combination of any of the quantities in $\mathbf{E}$.

The conditional eddy specifies a vector velocity field given an event. If the event is uniquely associated with the conditional eddy, then the probability of a conditional eddy is related one-to-one to the probability of $\mathbf{E}$. Thus, $< \mathbf{u}' \mid \mathbf{E} >$ gives the eddy shape and $f_{\mathbf{E}}$ gives the likelihood of occurrence. Unfortunately, the commonly used events such as quadrant analysis, VITA, and single point vectors do not guarantee a one-to-one relationship with a coherent structure. For example, a single coherent structure could have the same velocity vector at several points, or it could satisfy VITA or quadrant analysis criteria at several different points.

4.3 Properties of Linear Stochastic Estimates

The linear stochastic estimate of $< \mathbf{u}' \mid \mathbf{E} >$ shares many properties in common with the conditional eddy itself. Taking

$$\hat{u}_i' = A_i + L_{ij} E_j \tag{4.13}$$

where <**E**> is assumed to be zero, we see that (4.7a) follows immediately if $A_i = \langle u_i' \rangle$. (Recall that $L_{ij} = A_{ij}$). The reduction property (4.7b) is not, however, satisfied. The separation property (4.8), the coincidence property (4.9), and continuity (4.11) are each satisfied. To see that continuity is satisfied, take the divergence of $\hat{u}_i'$

$$\frac{\partial \hat{u}_i'}{\partial x_i'} = \frac{\partial L_{ij}}{\partial x_i'} E_j \tag{4.14}$$

From (3.3), the divergence of L_{ij} satisfies

$$\langle E_j E_l \rangle \frac{\partial L_{ij}}{\partial x_i'} = \left\langle \frac{\partial u_i'}{\partial x_i} E_l \right\rangle = 0 \tag{4.15}$$

But if (3.3) has solutions, then $\det < E_j E_l > \neq 0$, in which case the only solution of (4.15) is $\partial A_{ij} / \partial x_i' = 0$. Hence, $\partial \hat{u}_i' / \partial x_i' = 0$, as assured.

The continuity of the stochastic estimate of the conditional average is a very useful property. If means that the stochastic estimate is at the least a viable initial condition for the Navier-Stokes equation.

The essential difference between the conditional average and its LSE is the failure of the LSE to satisfy the reduction property (4.7b) in general. The special case $\mathbf{E} = \mathbf{u}(\mathbf{x})$ is an exception. The exact relationship for this case is

$$\langle u_i \langle u_j' \mid \mathbf{u} \rangle \rangle = \langle u_i u_j' \rangle. \tag{4.16}$$

The corresponding relationship obtained using the linear estimate of the conditional eddy is

$$\langle u_i L_{jl} u_l \rangle = L_{jl} \langle u_i u_l \rangle \tag{4.17a}$$

$$= \langle u_j' u_i \rangle \tag{4.17b}$$

where (4.17b) follows from (3.3). Hence the correct two-point spatial correlation function is retrieved identically from the LSE, as should be expected since the LSE takes the two-point spatial correlation function as input. For any other $\mathbf{Q}(\mathbf{E})$ the linear estimation does not guarantee reduction of <**Q**(**E**)<**u**'|**E**>> to <**Q**(**E**)**u**'>. This is important in regard to the use of LSE for closure approximations.

5. CONDITIONAL EDDIES AND COHERENT STRUCTURES

5.1 Isotropic Turbulence

Isotropic turbulence is defined by invariance of its statistics with respect to translations of the coordinate origin, reflections about planes through the origin and arbitrary rotations about the origin. It is understood to be the least structured of all turbulent flows. In this secton we shall summarize results concerning the structure of stochastically estimated eddies in isotropic turbulence. We will see that although the field is isotropic, the conditional eddies are anisotropic structures, owing to the imposition of anisotropic events.

The first studies of the structure of isotropic tubulence (Adrian 1979, Tung and Adrian 1980) concentrated on using the single-point velocity vector $\mathbf{E} = \mathbf{u}(\mathbf{x},t)$ to define the flow condition at $\mathbf{x}$. It was shown in general that the vector field of the conditional eddy $<\mathbf{u}'|\mathbf{u}>$ must be axisymmetric about $\mathbf{u}(\mathbf{x},t)$ for any isotropic turbulent flow. Linear stochastic estimates of $<\mathbf{u}'|\mathbf{u}>$ relate it approximately to the two-point spatial correlation, and they showed that the axisymmetric field has the form a vortex ring that is centered on $\mathbf{u}(\mathbf{x},t)$ and oriented with its plane perpendicular to it. Non-linear stochastic estimates revealed that corrections to the vortex ring due to higher order terms are significant only if the magnitude of the local velocity fluctuation $|\mathbf{u}(\mathbf{x},t)|$ is improbably large (Tung and Adrian 1980). For probable levels of the fluctuation the conditional eddy is a slightly perturbed vortex ring, suggesting a certain robustness of the ring structure in turbulence.

Ditter (1987) considered the conditional eddy given the local kinematics, defined by $<\mathbf{u}'|\mathbf{u},\mathbf{d}>$, the conditional average given both the velocity $\mathbf{u}(\mathbf{x},t)$ and the deformation tensor

$$d_{ij}(\mathbf{x},t) = \partial u_i / \partial x_j \tag{5.1}$$

Interest in this more complicated conditional event stemmed from the fact that $\mathbf{u}(\mathbf{x},t)$ and $\mathbf{d}(\mathbf{x},t)$ jointly specify the complete kinematic state of the fluid motion at $(\mathbf{x},t)$ in terms of the translation, rotation and rate-of-strain at that point. Consequently, more detailed and more accurate estimates of the surrounding structure were expected by virtue of having more copletely described the field at $(\mathbf{x},t)$. The following results draw heavily from the thesis of Ditter (1987) and Ditter and Adrian (1988).

In homogeneous turbulence the form of the linear stochastic estimate of $<u_i'(\mathbf{x}')\,|\,\mathbf{u}(\mathbf{x}),\mathbf{d}(\mathbf{x})>$ is

$$\hat{u}_i' = \hat{u}'(\mathbf{x}') \quad = A_{ij}u_j(\mathbf{x}) + B_{ijk}d_{jk}(\mathbf{x}), i,j,k = 1,2,3 \tag{5.2}$$

where $\mathbf{x}'$ is any point around $\mathbf{x}$, and the estimation coefficients $\mathbf{A}$ and $\mathbf{B}$ are functions of

$$\mathbf{r} = \mathbf{x}' - \mathbf{x} \tag{5.3}$$

for homogeneous turbulence. (Hereafter, the time dependence will be suppressed).

The linear stochastic estimate in (5.2) is obtained by expanding the conditional average $< \mathbf{u}'|\mathbf{u},\mathbf{d} >$ in a first order Taylor series about $\mathbf{u}(\mathbf{x}) = 0$ and $\mathbf{d}(\mathbf{x})=\mathbf{0}$ using the fact that the mean value <u> vanishes in isotropic turbulence to show that the constant term in the expansion is zero.

The coefficients in the expansion are determined, as usual, by minimizing the mean square errors, computed for each component of u_i' by averaging over all possible random values of **u** and **d**.

$$e_i = \left\langle [u_i' - \langle u_i' \mid \mathbf{u},\mathbf{d} \rangle]^2 \right\rangle = \min imum, \quad i = 1,2,3. \tag{5.4}$$

Setting $\partial e_i / \partial A_{i\ell} = 0$ and $\partial e_i / \partial B_{i\ell m} = 0$ *for* $i,\ell,m = 1,2,3$ leads to the following equations for **A** and **B**.

$$A_{ij}(\mathbf{r})\, R_{j\ell}(\mathbf{0}) + B_{ijk}(\mathbf{r})\, R_{\ell j,k}(\mathbf{0}) = R_{\ell i}(\mathbf{r}) \tag{5.5}$$

$$-A_{ij}(\mathbf{r})\, R_{lj,m}(\mathbf{0}) + B_{ijk}(\mathbf{r})\, R_{\ell j,km}(\mathbf{0}) = R_{\ell i,m}(\mathbf{r}) \tag{5.6}$$

for i,j,k, ℓ,m = 1,2,3. Here $R_{\ell j}(\mathbf{r})$ is the two-point spatial correlation tensor.

$$R_{\ell j}(\mathbf{r}) = <u_\ell(\mathbf{x})\, u_j(\mathbf{x}+r)>, \tag{5.7}$$

and

$$-R_{\ell j,k}(\mathbf{0}) = [-\frac{\partial R_{\ell j}}{\partial r_k}]_{\mathbf{0}} = < u_j d_{\ell k} > \tag{5.8}$$

$$-R_{\ell i,m}(\mathbf{r}) = [\frac{\partial R_{\ell i}}{\partial r_{m\,r}}]_{\mathbf{r}} = < u_i' d_{\ell m} > \tag{5.9}$$

$$-R_{\ell j,km}(\mathbf{0}) = [\frac{\partial^2 R_{\ell j}}{\partial r_k \partial r_m}]_{\mathbf{0}} = < d_{\ell m} d_{jk} > \tag{5.10}$$

give the correlations between the velocity and its derivatives in terms of $R_{\ell i}(\mathbf{r})$. Equations (5.5) and (5.6) constitute three independent sets (i=1,2,3) of twelve equations.

In isotropic turbulence $< u_\ell u_j > = u^2 \delta_{\ell j}$ where $u^2 = < u_i u_i > /3$ is the mean square fluctuation, and $R_{\ell j,k}(\mathbf{0}) = 0$ from reflectional invariance. Hence, (5.5) and (5.6) decouple, and the following solution for the first estimation coefficient is obtained from (5.5) immediately:

$$A_{il} = R_{\ell i}(\mathbf{r})/u^2. \tag{5.11}$$

This is exactly the same as the solution found for the linear estimate of $< u_i' | \mathbf{u} >$.

The solution for $B_{ijk}(\mathbf{r})$ is complicated by the fact that

$$d_{11} + d_{22} + d_{33} = 0 \tag{5.12}$$

in incompressible flow. Consequently, one of the nine components of the deformation data is statistically dependent on the others, and the system of equations for B_{ijk} does not yield unique solutions. The non-uniqueness in (5.12) is made evident by noting that incompressibility requires that $R_{\ell i,\ell}(\mathbf{r}) = 0$. Hence, one of the equations is linearly dependent. In Adrian and Moin (1988) the non-uniqueness of **B** was eliminated by deleting d33 from the list of data given at **x** and performing numerical solutions of (5.5) and (5.6) for all i,j,k, ℓ,m = 1,2,3 *except* ℓ=m=3, j=k=3. This approach is best for situations requiring numerical solutions, but in the present case, where analytical solution is possible due to the high degree of symmetry in the statistics of the flow, it is easier to carry d33 and obtain non-unique solutions for B_{ijk}.This non-uniqueness is not troublesome because it vanishes when B_{ijk} is combined with d_{jk} to form the estimate of velocity.

Using $R_{\ell j,m}(\mathbf{0}) = 0$, (5.6) reduces to

$$B_{ijk}\, R_{\ell j,km}(\mathbf{0}) = R_{\ell i,m}(\mathbf{r}). \tag{5.13}$$

For isotropic, incompressible turbulence the correlation on the left-hand side is given by

$$R_{\ell j,km}(0) = \begin{cases} -u^2/\lambda^2 , & j = k = \ell = m \\ -u^2/\lambda^2 , & \ell = m \neq j = k \text{ or } j = k \neq \ell = m \\ -2u^2/\lambda^2 , & k = \ell \neq j = m \\ 0 \quad . \quad \text{otherwise,} \end{cases} \tag{5.14}$$

where λ is the longitudinal Taylor microscale. The solution to (5.13) becomes

$$B_{ill}(\mathbf{r}) = \text{arbitrary}, \tag{5.15a}$$

$$B_{i22}(\mathbf{r}) = -\frac{\lambda^2}{u^2}\{\frac{4}{3}R_{2i,2}(\mathbf{r}) + \frac{2}{3}R_{3i,3}(\mathbf{r})\} \tag{5.15b}$$

$$B_{i33}(\mathbf{r}) = -\frac{\lambda^2}{u^2}\{\frac{2}{3}R_{2i,2}(\mathbf{r}) + \frac{4}{3}R_{3i,3}(\mathbf{r})\} + B_{ill}(\mathbf{r}), \tag{5.15c}$$

and

$$B_{i\ell m}(\mathbf{r}) = -\frac{2\lambda^2}{15u^2}\{R_{mi,\ell}(\mathbf{r}) + 4R_{\ell i,m}(\mathbf{r})\} \tag{5.15d}$$

for $\ell \neq$m. Details can be found in Ditter (1987).

The complete stochastic estimate is

$$\hat{u}_i(\mathbf{x}+\mathbf{r}) = \frac{R_{ji}(\mathbf{r})}{u^2}u_j(x) - \frac{2\lambda^2}{15u^2}\{R_{ki,j}(\mathbf{r}) + 4R_{ji,k}(\mathbf{r})\}d_{jk}(x). \tag{5.16}$$

In this equation the unknown function $B_{ill}(\mathbf{r})$, drops out of the product $B_{ijk}(\mathbf{r})\,d_{jk}(\mathbf{x})$ due to the incompressibility condition $d_{ii} = 0$. Each term in (5.16) can be evaluated in terms of the longitudinal correlation coefficient

$$f(r) = \langle u_1(\mathbf{x})u_1(\mathbf{x}+r\hat{\mathbf{e}}_1)\rangle / u^2 \tag{5.17}$$

by means of the isotropic relation (Batchelor 1986)

$$R_{ji}(\mathbf{r}) = u^2\{-\frac{1}{2}f'(r)\frac{r_i r_j}{r} + [f + \frac{1}{2}r\,f']\,\delta_{ij}\}. \tag{5.18}$$

The grid turbulence measurements of Van Atta and Chen (1968) were used to evaluate $f(r)$ at 48 mesh spacings downstream of a bi-plane grid. The mesh spacing was M= 25.4 mm and the conditions at $x_1/M = 48$ were u=0.24 ms^{-1}, L_{11} (longitudinal integral length scale) = 13 mm, λ = 3.9 mm, and $uL_{11}/\nu = 200$. For the results concerning large scale structure the longitudinal correlation coefficient $f(r)$ is represented adequately by the curve fit

$$r(r^*) = (1 - 0.435r^* + 0.188r^{*2}$$

$$-0.026r^{*3})\,e^{-0.626r^*} \tag{5.19}$$

where $r^* = r/L_{11}$. This representation is not valid for r less than approximately one Taylor microscale; but at large Reynolds number $\lambda/L_{11} \ll 1$, so the representation is accurate everywhere except in a small region about r = 0. (For Van Atta and Chen's experiment $\lambda/L_{11} = 0.3$ *at* $x/M = 48$. The longitudinal correlation coefficient f(r) and the associated transverse correlation coefficient g(r) are shown in Fig. 5.1. Note that the data of Van Atta and Chen are distinctive in that f(r) becomes negative at large separations, with the

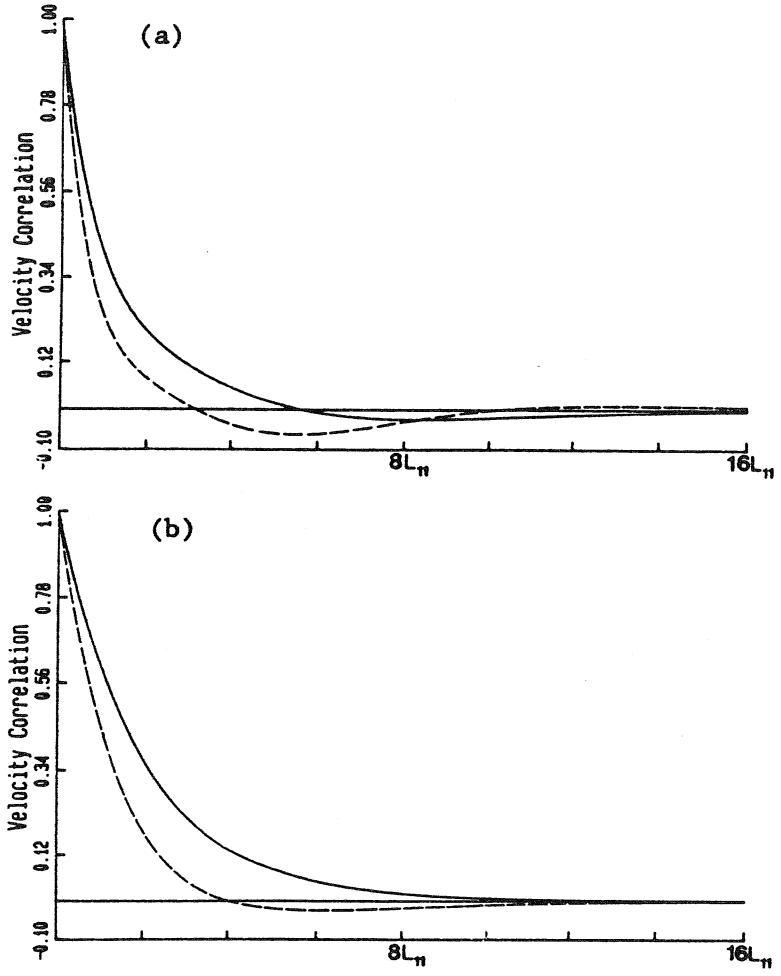

Figure 5.1 Velocity correlation data of Van Atta and Chen (1968): f(r)———; g(r) - - - - -.

consequence that g(r) has two zeroes. The implications of this behavior in regard to the structure of the conditional eddy $< \mathbf{u}'|\mathbf{u} >$ will be discussed shortly.

The results will be presented in terms of the following dimensionless variables:

$$u^* = \mathbf{u}/u, \mathbf{d}^+ = \lambda \mathbf{d}/u \tag{5.20}$$

$$R^*_{ij} = R_{ij}/u^2, \quad R^*_{ij,k} = L_{11}R_{ij,k}/u^2, \tag{5.21}$$

where $$\lambda = u/\sqrt{<(\partial u_1/\partial x_1)^2>}.$$

In terms of these variables,

$$\hat{u}_i^*(\mathbf{x}^*+\mathbf{r}^*) = R_{ji}(r^*)\,u_j^*(\mathbf{x}^*) - \frac{2\lambda}{15L_{11}}\{R^*_{ki,j}(\mathbf{r}^*) + 4R^*_{ji,k}(\mathbf{r}^*)\}\,d^+_{jk}(\mathbf{x}^*). \quad (5.22)$$

The non-dimensionalization of **d** by u/λ is chosen to make the elements of $\mathbf{d}^+$ of order unity when their dimensional values are of the order of the root mean square spatial derivative. The nondimensional derivatives of the correlation function $R^*_{ki,j}$ are of order one when r is of the order of the integral length scale.

5.2 Pure translation event

In pure translation, u(x) = (|u(x)|,0,0). and **d**(x) = **0**. The linear stochastic estimate is a pair of vortex rings centered on **x** and axisymmetric about **u**(x), Fig. 5.2. The outer ring is a consequence of the negative tail in van Atta and Chen's measurements of f(r). The core of the inner ring is centered on the first zero of the transverse correlation function, g(r), and the core of the outer ring is centered on the second zero of g(r). It moves off to infinity if the negative region of f(r) is reduced to zero, e.g., if f(r) decreases monotonically.

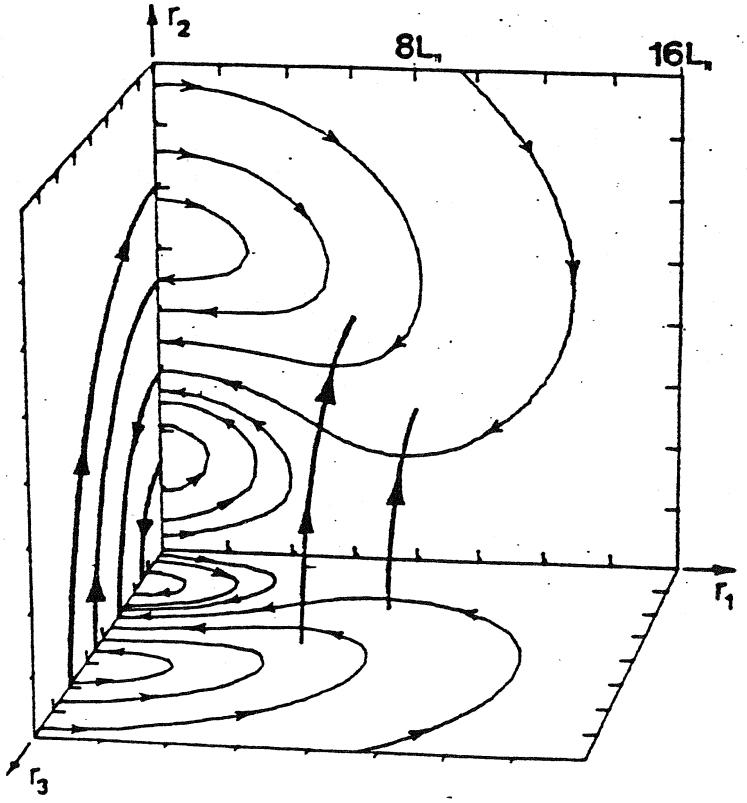

Figure 5.2 Conditional eddy given pure translation. Streamlines (light ink) and vortex lines (heavy ink).*[from Ditter and Adrian 1988].*

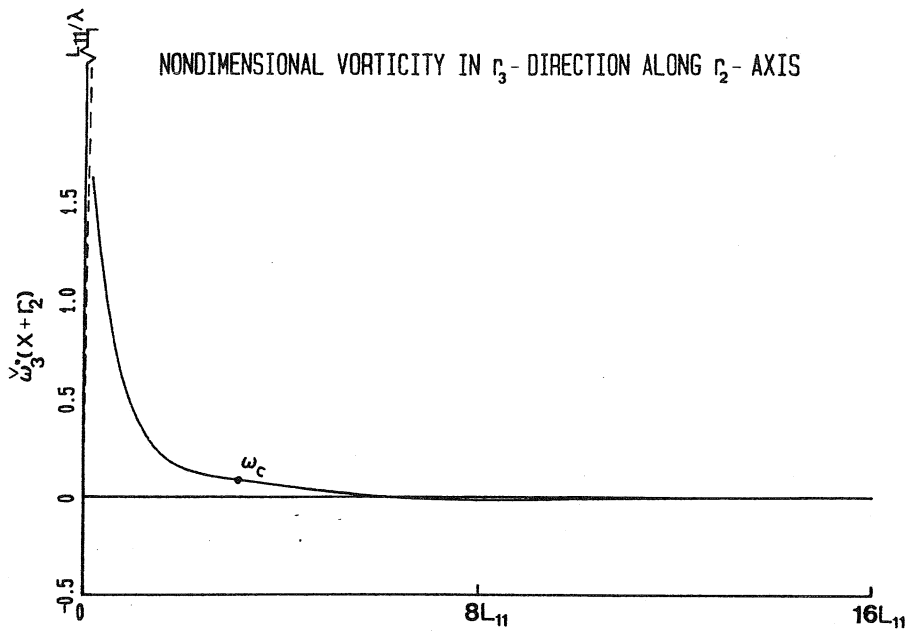

Figure 5.3 Distribution of $\hat{\omega}_3^*(\mathbf{x}+\mathbf{r})$ along the r_2 axis for a ring vortex conditioned on $\mathbf{u}(\mathbf{x}) = (u, 0,0)$. The dashed line is calculated from $f \doteq 1 - r^2/2\lambda^2$. The vorticity at the center of the inner vortex ring is ω_c. *[from Ditter and Adrian 1988].*

The magnitude of the velocity field within the inner ring is of the order of $\mathbf{u}(\mathbf{x})$, and if $\mathbf{u}(\mathbf{x})$ were strong a random realization similar to this field would be expected to be strong enough to persist as an organized motion, despite the presence of other random fields surrounding it. In contrast, the outer ring is much weaker. Because it is unlikely that such a weak structure could maintain itself for long against the disturbances of the surrounding random environment, it is perhaps more reasonable to interpret the inner ring as the mean field of an organized structure, and the outer ring as the mean of all of the other organized structures that surround it. The fact that the mean surrounding field is non-zero implies that there is an interaction between the inner vortex ring and surrounding organized structures which may, themselves, be ring-like.

The vorticity distribution along a radial line in the $r_2 - r_3$ plane of the ring is shown in Fig. 5.3. The solid line is calculated from (5.18), (5.19), and (5.22); it represents the high Reynolds number behavior of the large, inviscid scales of motion, $r_2 \sim L_{11} >> \lambda$. In this region, which covers most of the vortex ring, the vorticity scales with $u(\mathbf{x})/L_{11}$. For small values of r, the Taylor series expansion

$$f(r) = 1 - r^2/2\lambda^2 + \ldots \tag{5.23}$$

combined with (5.18) and (5.22) predicts that the vorticity varies like $5|\mathbf{u}(\mathbf{x})|/\lambda$. indicated by the dashed line in Fig. 5.3. The vorticity of the purely translational conditional eddy vanishes at r = 0, and increases rapidly to a maximum value before decaying according to the solid line

in Fig. 5.3. Subsidiary calculations using a more complete model of f(r) show that the maximum vorticity is of order u(x)/λ, and that it occurs at a radius of order λ. For small

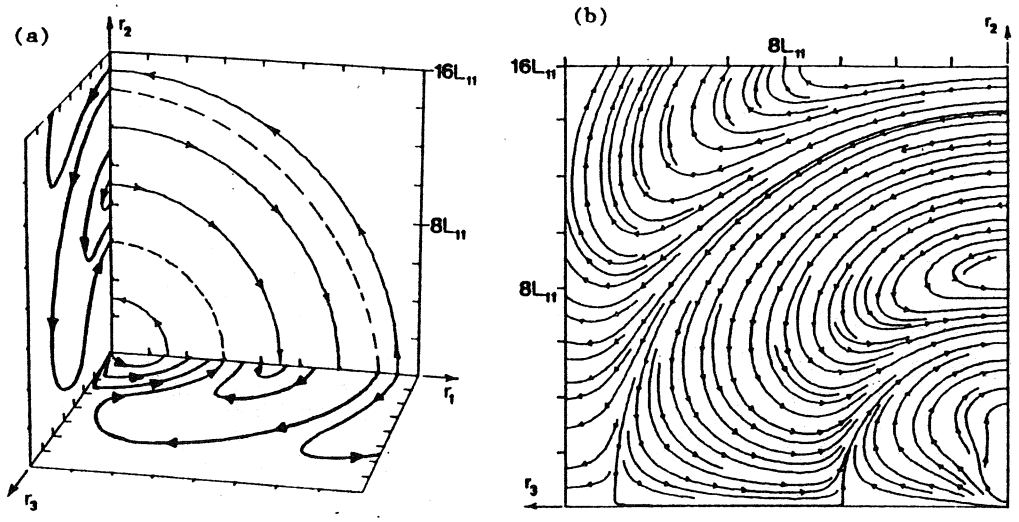

Figure 5.4 Conditional eddy given pure rotation about the r_3 axis: a) streamlines in $r_1 - r_2$plane and vortex lines in $r_1 - r_3$ and $r_2 - r_3$ planes demonstrating symmetry about r_3 – axis; b) vortex lines in $r_2 - r_3$plane. *[from Ditter and Adrian 1988].*

radii the flow is affected by viscous stresses, and the vorticity is primarily due to an axisymmetric shearing motion, as opposed to a circulating vortical motion. The ratio of the maximum vorticity to the vorticity in the core of the inner vortex ring, indicated by ω_c in Fig. 5.3, is proportional to L_{11}/λ. Thus, at low Reynolds the vorticity of the core is comparable to the maximum vorticity, whereas at high Reynolds number it is much less than the maximum, and most of the vorticity is concentrated in a region of radius λ. However, the *circulation* of the core of the ring is of order $[u(x)/L_{11}]L_{11} = u(x)$. Thus, it is comparable to the circulation of the small scale region, $[u(x)/\lambda]\lambda \sim u(x)$.

5.3 Pure deformation events

Four conditions in which the state of the flow at x is one of pure deformation are considered here: $u(x) = 0$ and $d(x) \neq 0$. They are pure rotation, Fig. 5.4; axisymmetric strain, Fig. 5.5; plane strain, Fig. 5.6; and plane shear, Fig. 5.7. In each oblique view the light lines indicate streamlines and the heavy lines indicate vortex lines.

The state of pure rotation about the r3-axis in Fig. 5.4 is given by $u(x) = 0$, $d_{12} = -d_{21} = -\omega_3(x)$, and $d_{ij}(x) = 0$, otherwise. The field is axisymmetric about r_3, and it consists of three counter-rotating shells. If vortex rings are the dominant organized structure in isotropic turbulence, one might expect that specifying the vorticity at x would place x on the

core of the ring with its *tangentially oriented* vorticity aligned with the given vorticity. However, merely specifying $\omega(x)$ is insufficient to identify the orientation of a ring; the

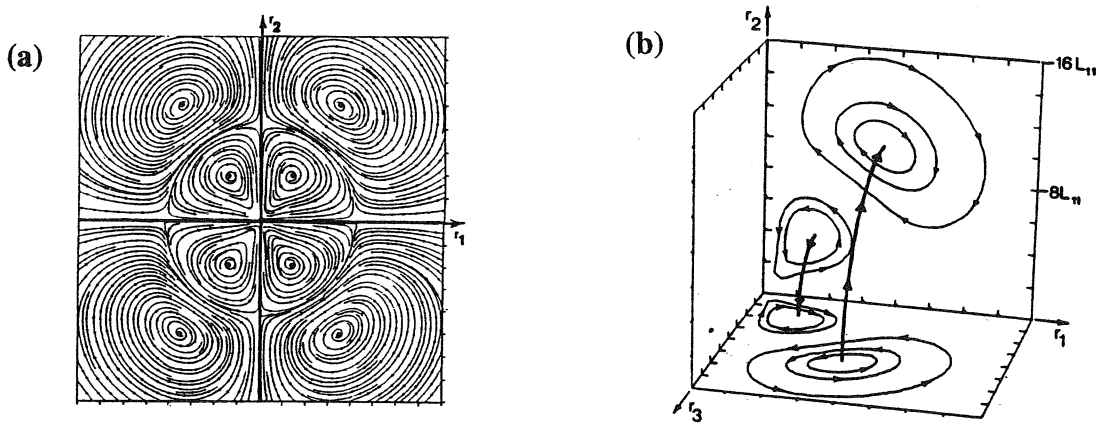

Figure 5.5 Conditional eddy given axisymmetric strain.(a) streamlines in $r_1 - r_2$ plane;(b)streamlines (light ink) in the $r_1 - r_2$ and $r_1 - r_3$ planes with vortex lines (heavy ink) demonstrating the axisymmetry of the flow about the r_1-direction.*[from Ditter &Adrian 1988].*

vorticity could correspond to any ring whose central velocity u(x) is perpendicular to $\omega(x)$. Thus, the conditional eddy is Fig. 5.4 is rotationally symmetric about ω, and corresponds, qualitatively, to an average of translational vortex rings rotated about $\omega(x)$.

Contours of constant$|\omega|$ for pure rotation indicate a long, rod-like zone of high vorticity aligned with the r_3 axis. The length of this rod is of order several integral length scales and its diameter is of order of the Taylor microscale. The strength of the vorticity in the rod is of the order of the given vorticity, while that outside of the rod, i.e., most of the region shown in Fig. 5.4, is of order $|\omega|\lambda/L_{11}$, i.e., much smaller. The intense rod-like structure may be related to the vortical "worms" that have been observed in direct numerical simulation of isotropic turbulence.

The state of pure axisymmetric strain at x with principal axis of positive extension aligned with the r_1-direction is given by $d_{11}(x) = -2d_{22}(x) = -2d_{33}(x)$. The velocity vector field is axisymmetric about the r_1-axis, Fig. 5, and it consists of four vortex rings. The two smaller rings create the axisymmetric strain at x, and the two outer rings are consequences of the negative tail of f(r).

Plain strain at x with the principal axis of positive extension laying in the $r_1 - r_2$ plane at 45° to the r_1-direction and the principal axis of compression lying at 135° is given by u(x) = **0** and $d_{12}(x) = d_{21}(x)$ with all other components of **d**(x) vanishing. In this case the

nature of **d** precludes axisymmetry but implies reflectional symmetry with respect to the r_1-r_2, $r_2 - r_3$ and $r_1 - r_3$ planes, and with respect to the planes at 45° and 135° to the r_1-axis. The flow consists of four inner vortical regions and four outer regions connected as shown by the vortex lines in Fig. 5.6.

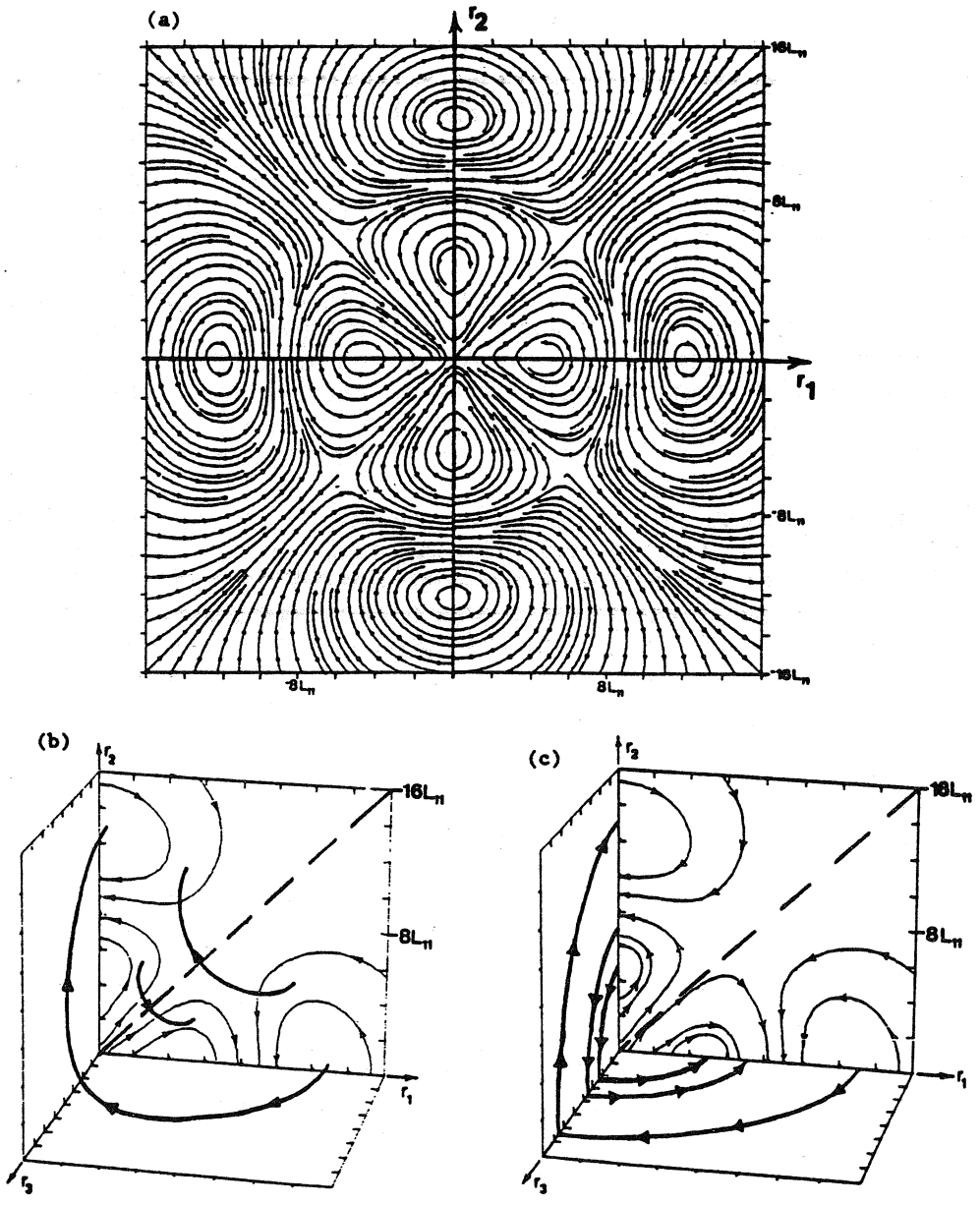

Figure 5.6 Conditional eddy given plane strain. a) streamlines in the $r_1 - r_2$ plane; b) streamlines (light ink) in the $r_1 - r_2$ plane and out-of-plane vortex lines (heavy ink); c), streamlines in the $r_1 - r_2$ plane and vortex lines in the $r_1 - r_3$ and $r_2 - r_3$ planes.*[from Ditter &Adrian 1988].*

6. CONDITIONAL EDDIES IN ANISOTROPIC TURBULENCE

In anisotropic turbulence, the correlation tensor and, hence, the linear stochastic estimate become more complicated and reflect the asymmetries of the flow. For example, in homogeneous shear flow the form of the conditional eddy is a hairpin vortex similar to that shown in Fig. 6.1 (Adrian and Moin 1988; Adrian 1990). If the fluctuating vorticity is given one of its most probable values, which is inclined at approximately 45° to the direction of the mean flow, the plane of the hairpin lies in the same direction. This is the direction of maximum straining motion, as expected. The hairpin pumps fluid by vortex induction in such a way that if the hairpin is inclined forward, it produces a second quadrant event, i.e., negative u--component and positive v-component. The maximum induced velocity is approximately perpendicular to the plane of the hairpin, and being large, it contributes substantially to the mean Reynolds shear stress. The hairpins may also be inclined negatively, in which case the vortex induction produces a fourth quadrant event. Hairpins such as these are observed in the instantaneous realizations of direct numerical simulations of turbulence by Rogers and Moin (1987), and their scale and geometry are mimicked well by the linear stochastic estimates computed by Adrian and Moin (1988). This comparison between the linear stochastic estimate and the hairpins observed in random realizations is one of the best pieces of evidence that the stochastic estimates, given a proper condition, are able to faithfully reproduce all of the salient aspects of a coherent structure.

The structure of conditional eddies in inhomogeneous anisotropic shear flow has been studied using direct numerical simulations of low Reynolds number turbulent channel flow (Adrian, Moin and Moser 1987; Moin, Adrian and Kim 1987; Kendall 1992) The three-dimensional database makes it possible to obtain the full two-point spatial correlation tensor.

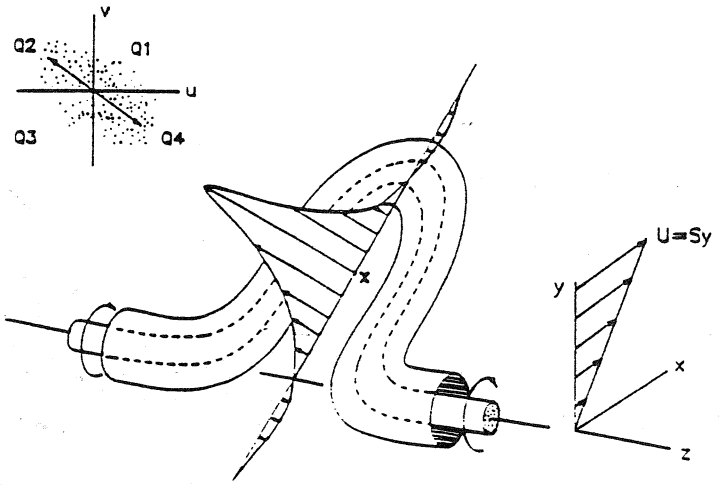

Figure 6.1 Inclined, hairpin-shaped conditional eddies in homogeneous shear flow induce flows that create strong Reynolds stress events in the second and fourth quadrants.*[from Adrian 1990].*

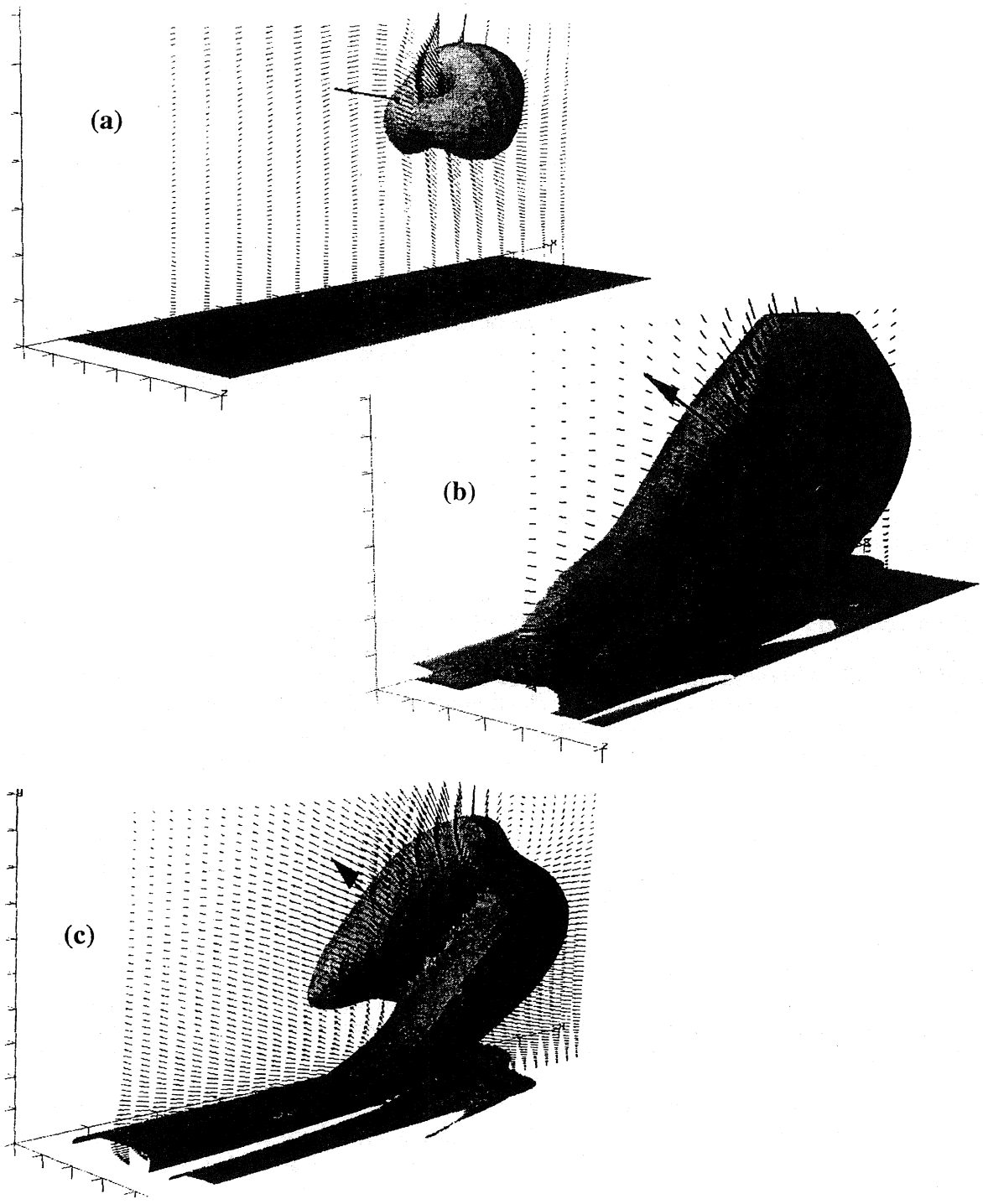

Figure 6.2 Conditional eddies in low Reynolds number turbulent channel flow estimated given a single-point conditional event $\mathbf{u}(\mathbf{x})$. Surfaces correspond to constant enstrophy fluctuation. Given vectors are the second quadrant events that correspond to the maximum contribution to the mean Reynolds shear stress. (a) $y^+= 180$ (channel centerline); $\mathbf{u}^+=(-0.81, 0.07, 0)$; (b) $y^+=103$, $\mathbf{u}^+=(-1.76, 1.1, 0.0)$; (c) $y^+=103$, $\mathbf{u}^+=(-1.76, 1.1, 2.0)$.

The results of the stochastic estimation based on a second-quadrant velocity vector event at a single point indicate an inclined hairpin structure with long quasi-streamwise vortical legs extending upstream from the inclined hairpin, such as those shown in Fig. 1.4 (y^+=49) and Fig.6.2(b) (y^+=103). In these figures the fluctuating magnitude of the vorticity is constant on the surfaces. The vectors denote velocity, and the heavy vector is the given velocity. The values of the velocity given in the caption to Fig. 6.2(b) correspond to the maximum probable contribution to the mean Reynolds stress. Very close to the wall the hairpin is not evident, and the primary feature of the conditional eddy is two long, counter-rotating, quasi-streamwise wall vortices. Farther away from the wall, the hairpin inclines upwards at a greater angle, and ultimately, on the centerline of the channel, where the mean shear is zero, the hairpin transforms into a simple vortex ring as shown in Fig. 6.2(a) (y^+=180). The inclined hairpin vortices on the wall induce low momentum flow to move upwards as do the long streamwise vortices behind the hairpin. This low momentum flow away from the wall creates strong Q2 events which are a dominant contributor to the mean Reynolds shear stress, $-\langle uv \rangle$ in the near wall region. The similarity between the hairpin in the wall layer and the hairpin in the homogeneous shear flow is noteworthy. However, in the wall flows, the quasi-streamwise vortices behind the hairpins are also very important in the creation of Reynolds shear stress.

Within the accuracy of linear estimation, specifying a Q4 event instead of a Q2 event simply reverses the sign of the velocity vector field of the conditional eddy. Thus, given a sweep event, the form of the conditional eddy is just an inclined hairpin with down-flow toward the wall. Although the fluctuating field is modified in a trivial way by such a sign change, the sum of the mean field plus the fluctuating conditional eddy field is different for the Q2 event relative to the Q4 event. This is particularly important when the fluctuation is strong enough for the non-linear interaction between the mean flow and the fluctuation to be important, for then sign difference will matter.

One of the criticisms of the stochastically estimated hairpin structure found from a Q2 event is that it is symmetric with respect to x-y plane through the center of the event. Robinson (1991) has noted that symmetric hairpin vortices are seldom observed in realizations of direct numerical simulations of turbulent channel flow and boundary layer flow, and statistical analysis by Guezennec, Piomelli and Kim (1987) has shown that hairpins are often asymmetric in nature, having circulation around one leg that is stronger than around another. The question is whether this sort of behavior can be obtained from stochastic estimation which is based on an inherently symmetric two-point spatial correlation tensor. In fact, one-legged hairpins are readily created from stochastic estimation by including a non-zero w-component of velocity in the conditional vector event. The effect of the non-zero w-component of velocity is to create a flow in the z-direction which generates a shear that has an x-component of vorticity. This x-component of vorticity intensifies one leg of the hairpin and weakens the other. The result is as shown in Fig. 6.2(c), which has been computed from the turbulent channel flow direct numerical simulation.

As well as their kinematics, the dynamics of conditional eddies are also important. While the conditional eddy is extracted from the physically based spatial correlation tensor, there is no guarantee that this structure is a stable structure, or that it does not quickly evolve into some other type of structure. For the case of turbulent channel flow at low Reynolds number discussed above, the dynamics of the eddies have been studied by Kendall (1992) and Zhou, Adrian and Balachandar (1995), by using the linear stochastically estimated vortex

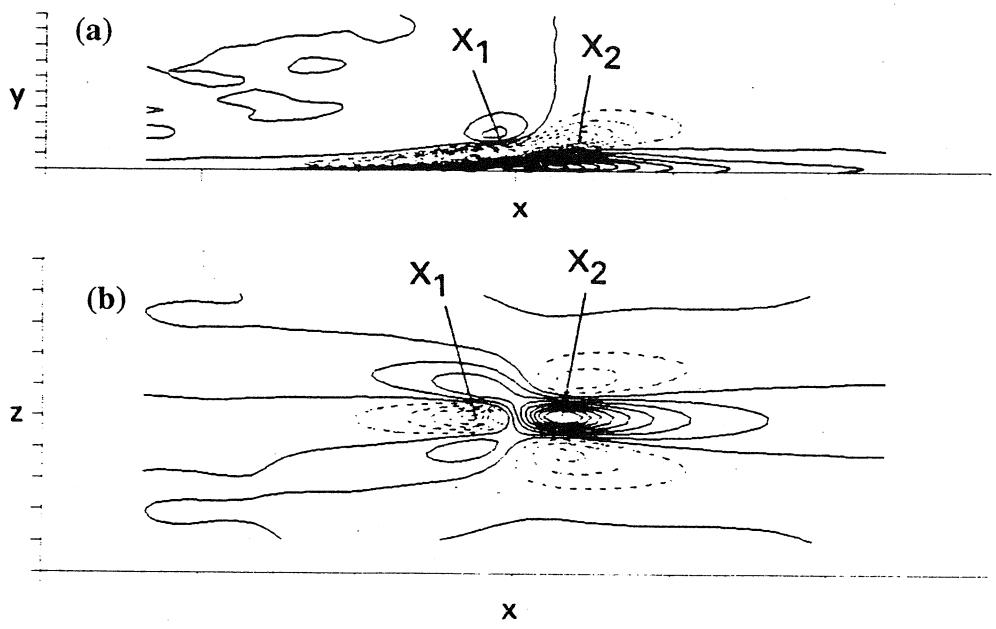

Figure 6.3 Linear estimation of channel flow given a Q2 event at $\mathbf{x_2}$ and a Q4 event at $\mathbf{x_1}$. (a) Contours of ω_z in the plane passing through $\mathbf{x_1}$. (b) Contours of the v-component of velocity in the x-z plane passing through $\mathbf{x_1}$. Solid line denote positive values.*[from Adrian, Moser and Moin 1987].*

as an initial condition and computing its evolution with time in a turbulent channel flow. The computations take the eddy in combination with the mean turbulent velocity profile. The results indicate that eddies whose conditional vector is less than approximately one rms velocity fluctuation in strength evolve very slowly after a brief transient from the initial conditional eddy into a slight sharper hairpin. After the transient, the eddy remains stable for several hundred viscous time units, which is more than long enough to contribute substantially to the mean time statistics. During this time the eddies sometimes grow slightly, but then generally decay slowly, while continuing to hold the shape of an initial conditional hairpin. More recent work by Zhou, Adrian, and Balachandar (1995) indicates that at sufficiently high intensity the initial hairpin vortex undergoes nonlinear evolution and begins to spawn further hairpin vortices.

One of the deficiencies of the hairpins estimated by specifying a single point Q2 vector event is that they do not exhibit the shear layer that is observed in direct numerical simulations and in experimental work to lie above and to the back of the hairpin vortex. This shear layer is an interaction between the slow, upward-moving fluid induced to flow between the legs of the hairpin, and faster, sweep-like fluid motions that approach the hairpin from behind. In order to observe this sort of flow field in the stochastic estimate, Adrian, Moser, and Moin (1987) and Guezennec (1989) imposed a two-point event which was a Q2 event at a point $\mathbf{x_2}$, as in Fig. 6.2, with a Q4 event slightly upstream of it at a point $\mathbf{x_1}$. The net effect was to create a shear layer very similar to that observed in the direct numerical simulations. We note that this combination Q2-Q4 event could also have been specified in effect by specifying a stagnation-point flow for the deformation tensor with a velocity vector of zero fluctuation intensity. An example of the Q2-Q4 combination event is shown in Fig. 6.3.

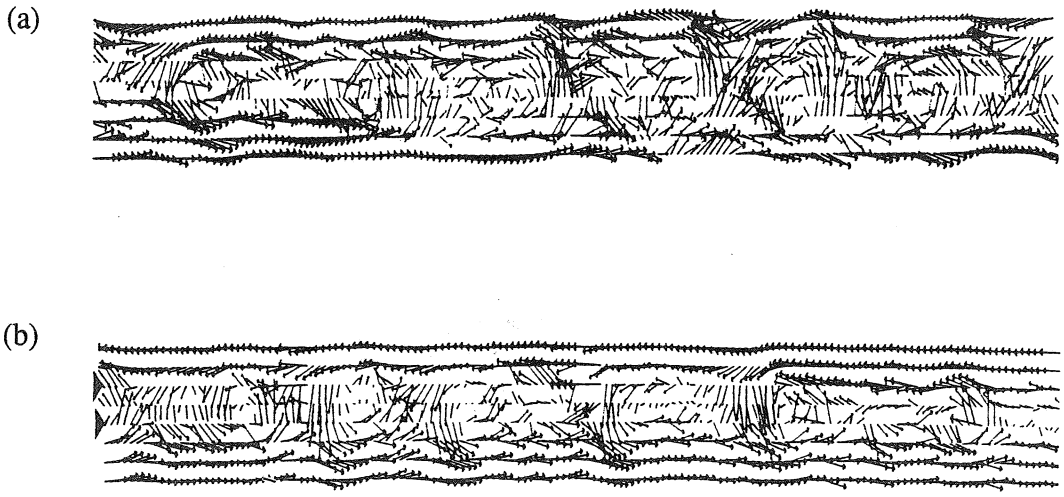

Figure 6.4 (a) Velocity vectors along horizontal lines in the shear layer of a round jet; (b) stochastically estimated field given data along the two line indicated by the arrows.*[From Ukeiley, et al. 1993].*

In turbulent shear layers, the linear stochastic estimate, given a velocity vector in the streamwise cross-normal plane at a single point, indicates spanwise roll cells in the fully turbulent zone of the turbulent shear layer (Tung 1980). Similar but much richer results are found in the shear layer of a turbulent jet by Cole, Glauser and Guezennec (1992). In this latter study the conditional event consisted of the time series of sampled velocity vectors at two radial locations bracketing the shear layer. Within the accuracy of Taylor's hypothesis the time series corresponded to sampling along two streamwise lines, which are indicated in Fig. 6.4. Comparison of the instantaneous realization in Fig.6.4(a) to the linear stochastic estimate in Fig.6.4(b) shows broad agreement. The stochastic estimate is somewhat smoother, indicating a low pass filtering effect, and the estimated fields decrease more rapidly than the realizations in the normal direction to the shear layer.

Roll cells in a turbulent wake have been studied by Gieseke and Guezennec(1993), using stochastic estimation given a single vector, Fig. 6.5. The flow pattern takes the form of two pairs of inclined vortices, which agrees rather well with the double roller model inferred from the correlation functions (Townsend 1976). Another way to view the conditional eddy is as a vortex ring that has been folded about a line in the streamwise-spanwise (x-z) plane. combined with time series of velocity vectors. Gieseke and Guezennec(1993) also used a time series along a line in the x-z plane to form a time-varying estimate of the velocity field given instantaneous data along the lines. The creation of a time varying depiction of the flow field in this way is similar to the work of Hassan (1980) in pipe flow, except that the latter estimates used only time varying data at one-point. From the line samples in time, Gieseke and Guezennec(1993) were able to predict a time-varying stochastic estimate which showed the translation and evolution of coherent structures in the wake. The results indicate inclined roller vortices. The movies show how the double roller structures interact in as they move. It is remarkable that fields of this complexity, c.f. Fig. 6.6, can be inferred from a single set of

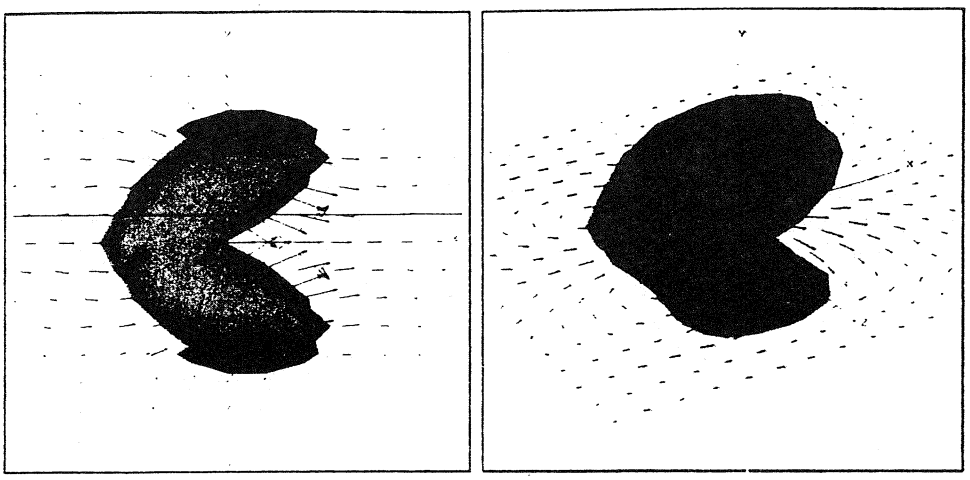

Figure 6.5 Stochastically estimated velocity field and surface of constant vorticity magnitude given Q2 event below the centerline and a Q4 event above the centerline of a turbulent wake. *[From Gieseke and Guezennec 1993].*

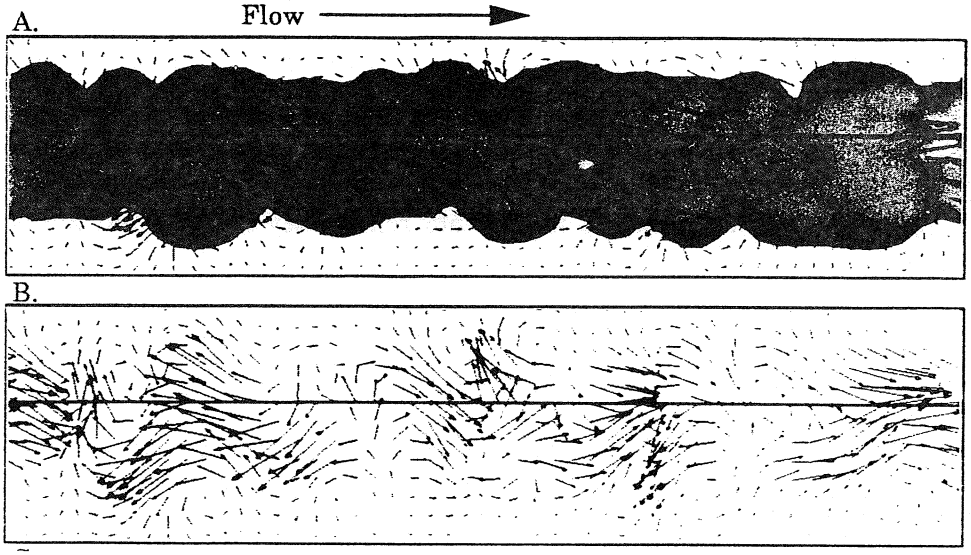

Figure 6.6 Estimated field constructed from a time series. Side view of surface of constant enstrophy.*[From Gieseke and Guezennec 1993].*

correlation function data almost as easily as fields given the velocity at say, one or two points.

Turbulent thermal convection between uniform, horizontal planes should have statistics that are symmetric with respect to rotations about the vertical direction of the gravitational vector. This symmetry occurs in the presence of strong inhomogeneity in the vertical direction. It is known from physical observations that the flows in thermal convection often take the form of plumes hot (or cold) fluid that rise(or fall) across the horizontal layer,

or unsteady, mushroom shaped thermals that occur in transient fashion as fluid moves away from one of the planes. At low Rayleigh numbers it is also known that convective roll cells form which are nearly two-dimensional. Interestingly, all of these phenomena can be observed by stochastic estimation, but only if the conditional event is chosen carefully (Balachandar and Adrian 1993). For example, stochastic estimation given a positive vertical velocity and a warm temperature fluctuation should give a roll cell or a thermal. In fact, unless the point for the event is very close to the surface, the flow is a large vortex ring that spans the fluid layer with its axis pointing vertically. After a little reflection it is clear that this shape is almost inevitable because an event that is axisymmetric about the vertical coupled with a two-point spatial correlation that is axisymmetric about the vertical must yield an estimated flow field with the same axisymmetry. How then can stochastic estimation ever predict two-dimensional roll-cells in such a flow? The answer is that one must use multi-point events to impose the two-dimensionality. Alternatively, but equivalently, one can work in both physical space and wavenumber space, using the latter to specify a two-dimensional event.

The stochastic estimate given a warm, rising event at one point is essentially an axisymmetric plume for all locations of the event except those very close to the horizontal boundaries, where the conditional eddy takes the form of an axisymmetric thermal with the characteristic mushroom-shaped head. This weaker flow field can also be found further away from the boundaries if one first estimates the large-scale roll-cell using a datum far from the wall, then subtracts the large scale field to obtain the smaller scale thermal field. This process is effective in extracting small eddies embedded in the fields of larger, stronger eddies.

In summary, for inhomogeneous and anisotropic flow fields, the linear stochastic estimate yields structures that are very similar to the flow structures observed in reality, provided that the given data reflect the important characteristics of the structures. The results are not very sensitive to the data, if they are reasonably chosen, but neither are they insensitive.

7. NEW DIRECTIONS IN STOCHASTIC ESTIMATION

New developments in the theory of stochastic estimation are being made on several fronts, most of them having to do with the intelligent selection of given events and/or optimization criteria. Developments are also being made in the application of stochastic estimation to a variety of turbulent flow problems.

Compared to modal decomposition methods that have global basis functions, like proper orthogonal decomposition, one of the strengths of stochastic estimation is that it yields fields that are compact in space if the events are located in a compact region (certainly this is true for single point events). By virtue of their compactness such fields can be viewed as representing eddies. However, from the viewpoint of interpolation and extrapolation, the fact that the fields decay with distance from the conditional events implies a loss of accuracy. The reduced energy is evident in Fig.6.4(b) compared to Fig.6.4(a). Cole, Glauser and Guezennec (1992) view this as a loss of signal energy and suggest that proper location of the event data can reduce the effect. Leboeuf and Mehta (1994) go further and recast the mean square error minimization problem as one in which the loss of energy of the signal is minimized. The resulting estimation problem is no longer linear, but the non-linear algebraic

equations are not difficult to solve. The solution effectively amplifies the decaying correlation functions to enhance their magnitudes at large distances from the event data. The process can enhance the signal, but there is clearly a limit to this process, as the loss of correlation that occurs with increasing separation between the event data and the estimated fields is real, and cannot be replaced by amplifying small numbers.

Closure of the pdf equations requires closure of conditional averages of the velocity and the Reynolds stress. Linear estimation can be used for the conditional eddy terms, but a different sort of approximation is needed for the conditional Reynolds stress. This problem is much like the closure for the unconditional Reynolds stress, except that the only place that the conditional Reynolds stress appears in the pdf equations is in the non-linear part of the pressure term, i.e. the slow pressure term. Efforts to approximate this term and to experimentally evaluate their success have been made by Tung (1980) and Elam (1987). Chang (1985) also measured the conditional pressure term and its stochastic estimate directly in the shear layer of an axisymmetric jet.

The problems of large eddy simulation are naturally phrased in terms of stochastic estimation. In Adrian (1977) and later in (Adrian 1990) the sub-grid scale closure problem was formulated as one of estimating the subgrid scale stresses given data in the form of the resolved scale field. It was shown that an 'optimal" algorithm could be developed that was optimal in the sense that it minimized the mean square error involved in the estimate of the time-rate-of-change derivative at each time step given the available grid data. For the usual large eddy formulation in which the resolved scales field is defined by a low pass filtering operation, the best estimate of the sub-grid scale Reynolds stresses was shown to be the conditional average of the SGS stresses given the large scale field. In this sense it is not

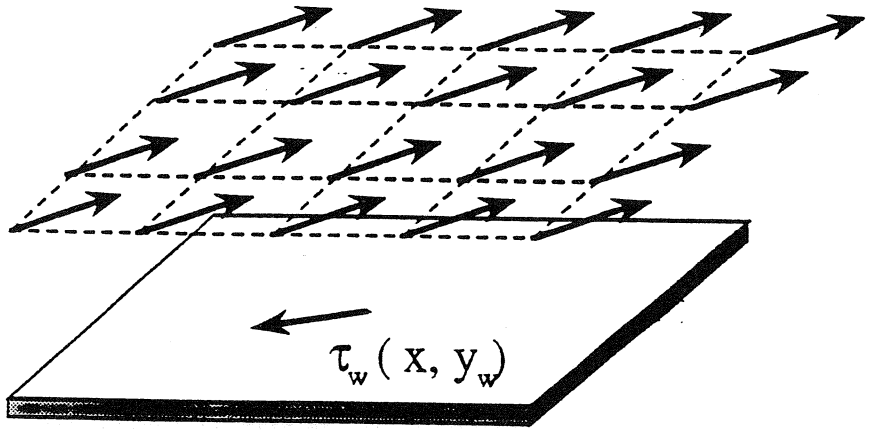

Figure 7.1 Stochastic estimation of the wall shear stress given velocity data on a neighboring numerical grid plane.

necessary to develop a relationship between the instantaneous SGS stresses and the instantaneous resolved scale field, explaining, perhaps, why the well known lack of correlation between these quantities does not have graver consequences for the closure approximations that are used in large eddy simulation.

A related problem in stochastic estimation is that of formulating a boundary condition for the resolved scale field in the wall region of a large eddy simulation. The boundary conditions that have been used are often ad hoc, and usually have little physical motivation. The work by Piomelli (1987) and Schumann (1975) expresses the wall shear stress in terms of the velocity of the resolved scales at the grid point closest to the wall. Schumann (1975) takes the point immediately above the wall location, while Piomelli (1987) takes a downstream point located so as to maximize the correlation between the wall shear stress and the grid velocity. Either boundary condition can be viewed as a linear estimate of the wall shear stress given the grid velocity datum.

These efforts suggest a generalized formulation of the problem in which all of the velocities computed on the first grid plane above the wall are used to estimate the wall shear stress as a function of position on the wall. c.f. Fig. 7.1. Note that the estimated field of wall shear stress is fully two-dimensional and time-dependent since the resolved scale data are evolving in time. This approach has been evaluated by Bagwell, Adrian, Moser and Kim (1993) using data from direct numerical simulation of channel flow to provide the correlation

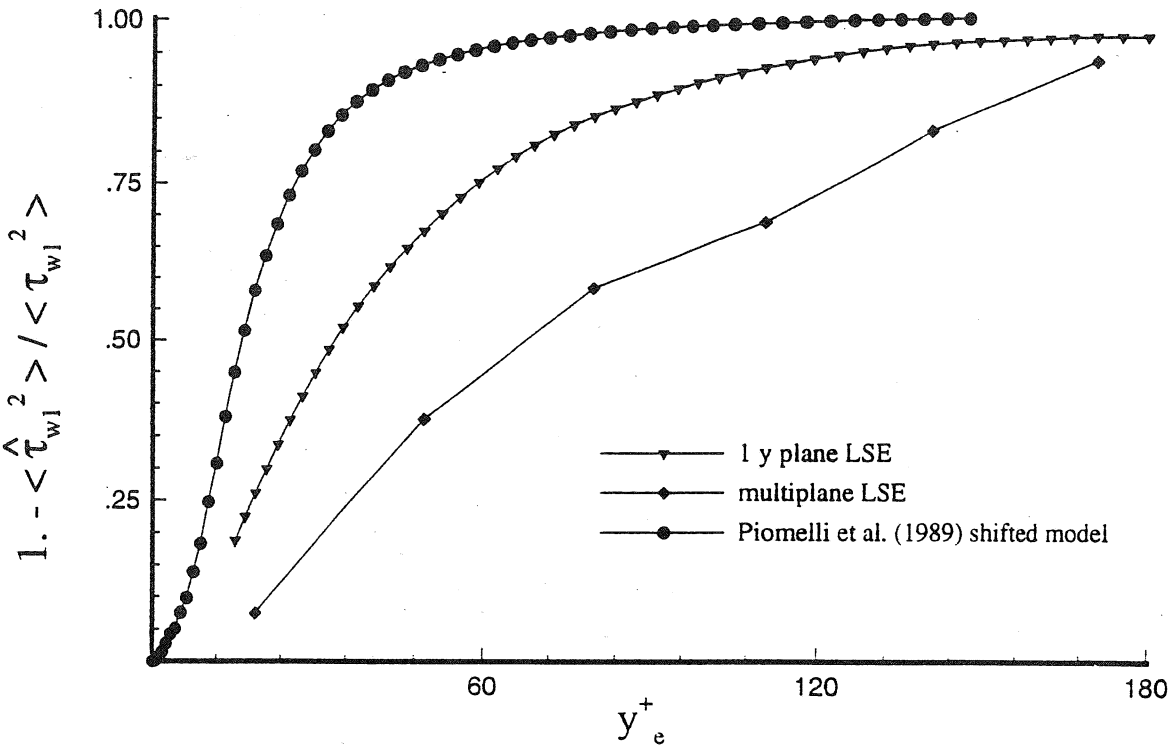

Figure 7.2 Relative mean square error in the estimate of the wall shear stress. *[from Bagwell, Adrian, Moser and Kim 1993].*

function used in the estimate and the data used to make a evaluation of the mean square error of the linear estimate. The results, shown in Fig. 7.2, indicate the mean square error for the wall shear stress as a function of the location y_e of the grid plane used for the data. Clearly the error must vanish as the grid plane approaches the wall. The error of the linear stochastic estimate is uniformly less than that of Piomelli's estimate, as should be the case because much more data is used in forming the estimate. When the value of y_e^+ exceeds about 30, the error approaches one-hundred per cent because the grid plane data become uncorrelated with the wall shear stresses. Further simulations were conducted by Bagwell (1994) to ascertain the effectiveness of this scheme when the computation of the resolved scale flow was coupled dynamically to the linear stochastic boundary condition. Results were stable and gave improved computations relative to earlier boundary conditions. Extensions to different Reynolds numbers require improved understanding of the scaling of the two-point spatial correlation function in the near-wall region, and extension to complex flow conditions requires an even greater generalization of the empirical representation of the correlation function.

The relationship between linear stochastic estimation and proper orthogonal decomposition (POD) continues to be an interesting topic of investigation. Both methods take the two-point correlation function as input, and it therefore appears at first glance as though they must be related. This is, of course, true, and under certain simplifying assumptions relations can be obtained. For example Berkooz, et al. (1993) consider joint normal random processes. Since the stochastic estimate is exactly equal to the conditional average in this case, they are able to develop several interesting relationships. However, in the general case the relationships between POD and LSE are not simple. For example, there is no simple relationship between a POD eigenmode and a conditional eddy. The eigenmode has a region of support that extends over the entire space of the decomposition, while the conditional eddy is compact. This is particularly obvious in homogenous turbulence where the eigenmodes from POD are simply trigonometric functions that individually carry no special information about the structure of turbulence. The LSE, on the other hand is capable of extracting structure regardless of the homogeneous state of the turbulence.

Since they form an orthogonal basis the correct way to use the POD eigenmodes in structural studies is to construct the structure from superposition of groups of the modes. The structure can be exactly represented by the superposition, and this is the strength of POD. In contrast LSE only approximates a structure locally. If greater accuracy is needed from a linear estimate, it is necessary to add more event data. It can be shown that there is a sampling theorem for linear stochastic estimation which shows that the linear stochastic estimate of a random function becomes exact if the data are sampled on a uniformly spaced grid and the sample spacing approaches the Nyquist sampling frequency. In fact, in the limit of Nyquist sampling the linear estimation coefficients exactly equal the sinc function specified in the Shannon Sampling Theorem. Thus, both linear estimation and POD become uninteresting when applied to fully sampled stationary random function.

The more interesting applications occur when the number of POD modes is limited so as to represent only a part of the signal or the number of event data are limited, corresponding to partial information for the stochastic estimate. In this regard Bonnet, et al. (1994) have recently combined POD and stochastic estimation by performing estimates of partial sums of POD modes and by examining estimation of the POD Fourier coefficients.

8. Summary and Conclusions.

Stochastic estimation is the approximation of a random variable in terms of given information. The best stochastic estimate is the conditional average. It has been shown that the conditional average itself can be estimated in terms of the data and the correlation functions between the data and the variable being estimated. The power of this result lies in the fact that once the estimation coefficients are found, the values of the event can be varied at will, making it possible to fully explore the space of events. A related property is that it is relatively easy to construct very complex events from sets of relatively simple data, again making it possible to explore a large class of events without having to perform conditional sampling

Acknowledgement

This work was supported by grants from the Office of Naval Research and the Air Force Office of Scientific Research. The assistance of R. Moser is greatly appreciated.

References

Adrian, R. J. (1977) On the role of conditional averages in turbulence theory. In J. Zakin and G. Patterson, Eds. *Turbulence in Liquids*. Princeton, NJ: Science Press, 323-332.

Adrian, R. J. (1979) Conditional eddies in isotropic turbulence. *Phys. Fluids* **22**, 2065-2070.

Adrian, R. J., Moin, P., Moser, R. D. (1987) Stochastic estimation of conditional eddies in turbulent channel flow, in: Moin, P., Reynolds, W. R., Eds. *Proc. of the 1987 Summer Program of the Center for Turbulence Research*, CTR-S87. NASA Ames Research Center, Moffett Field, CA, 7-20..

Adrian, R. J., Moin, P. (1988) Stochastic estimation of organized turbulent structure: homogeneous shear flow. *J. Fluid Mech.* **190**, 531-559.

Adrian, R. J., Jones, B. G., Chung, M. K., Hassan, Y., Nithianandan, C. K., Tung, A. T.-C. (1989) Approximation of turbulent conditional averages by stochastic estimation. *Phys. Fluids A.* **1**, 992-998.

Adrian, R. J. (1990) Linking correlations and structure: stochastic estimation and conditional averaging. in: Kline, S. J., Afgan, N. H., Eds. *Near Wall Turbulence, Proc. Zaric Memorial Intl. Symp.*, Washington D.C.: Hemisphere, 430-436.

Adrian, R. J. (1990) Stochastic estimation of sub-grid scale motions. *Appl. Mech. Rev.* **43**, 5214-5218.

Bagwell, T. G., Adrian, R. J., Moser, R. D., Kim, J. (1993) Improved approximation of wall shear stress boundary conditions for large eddy simulations. In: So, R., Launder, B., Eds. *Near Wall Turbulent Flows*. Amsterdam: Elsevier Science, 265-275.

Bagwell, T. G. (1994) Stochastic Estimation of Near Wall Closure in Turbulence Models. Ph. D. thesis, Univ. Illinois, Urbana, Illinois.

Balachandar, S., Adrian, R. J. (1993) Structure extraction by stochastic estimation with adaptive events. *J. Theoret. Comput. Fluid Dyn.* **5**, 243-257.

Batchelor, G. K. (1986) *The Theory of Homogeneous Turbulence*, Cambridge Univ. Press, Cambridge.

Berkooz, G.,Elezgaray, J., Holmes, P. Lumley, J. and Poje, A. (1993) The proper orthogonal decomposition, wavelets and modal approaches to the dynamics of coherent structures, In: Bonnet, J. P., Glauser, M. N., Eds. *Eddy Structure Identification in Free Turbulent Shear Flows*. Dordrecht: Kluwer. 325-336.

Brereton, G. J. (1992) Stochastic estimation as a statistical tool for approximating turbulent conditional averages. *Phys. Fluids A* **4**, 2046-2054.

Bonnet, J. P., Cole, D. R., Delville, J., Glauser, M. N., Ukeiley, L. S. (1994) Stochastic estimation and proper orthogonal decomposition: Complementary techniques for identifying structure. *Exp. Fluids* **17**, 307-314.

Chang, P. J. (1985) Fluctuating Pressure and Velocity Fields in the Near Field of a Round Jet. Ph.D. thesis, Univ. Illinois, Urbana, Illinois.

Chang, P. J., Adrian, R. J., Jones, B. G. (1985) Fluctuating pressure and velocity fields in the near field of a round jet. Univ. Illinois, Urbana, Illinois, Theo. & Appl. Mech. Report No. 475, UILU-ENG 85-6006.

Cole, D. R., Glauser, M. N., Guezennec, Y. G. (1992) An application of the stochastic estimation to the jet mixing layer. *Phys. Fluids A* **4**, 192-194.

Ditter, J. L. (1987) Stochastic Estimation of Eddies Conditioned on Local Kinematics: Isotropic Turbulence. M.S. thesis, Univ. Illinois, Urbana, IL.

Ditter, J.L. and Adrian, R.J. (1988). "Local flow structures around kinematic events in isotropic turbulence," presented at 11th Symp. on Turbulence, October 17-19, 1988, Univ. of Missouri-Rolla.

Deutsch, R. (1965) *Estimation Theory*. New York: Prentice-Hall, 1965.

Elam, K. S. (1987) Conditional Reynolds Stresses in the Near Field of a Round Jet. M.S. Thesis, Univ. Illinois, Urbana, Illinois.

Gieseke, T. J., Guezennec, Y. G. (1993) Stochastic estimation of multipoint conditional averages and their spatio-temporal evolution. in: Bonnet, J. P., Glauser, M. N., Eds. Eddy *Structure Identification in Free Turbulent Shear Flows*. Dordrecht: Kluwer, 281-292. ISBN: 0-7923-2449-8.

Guezennec, Y., Piomelli, U., and Kim, J. (1987) in *Proc. 1987 Summer Program of Center for Turbulence Research*, NASA Ames/Stanford Univ., Stanford, CA 263.

Guezennec, Y. (1989) Stochastic estimation of coherent structure in turbulent boundary layers. *Phys. Fluids A* **1**, 1054.

Hassan, Y. A. (1980) Experimental and Modeling Studies of Two-Point Stochastic Structure in Turbulent Pipe Flow. Ph.D. thesis, Urbana, IL: Univ. Illinois.

Johnsen, H., Pecseli, H. L., Trulsen, J. C. (1985) Conditional eddies, or clumps, in ion-beam-generated turbulence. *Phys. Rev. Lett.* **55**, 2297-2300.

Johnsen, H., Pecseli, H. L., Trulsen, J. C. (1986) Conditional eddies in plasma turbulence. *Plasma Physics and Controlled Fusion* **28**, 1519-1523.

Kendall, T. M. (1992) Dynamics of Conditional Vortices in Turbulent Channel Flow: A Direct Numerical Simulation. M.S. thesis, Univ. Illinois, Urbana, Illinois.

LeBoeuf R. L., Mehta, R. Improved methods for linear estimation of velocity records. *Exp. Fluids* **17**, 32-38.

Lundgren, T.S. (1967) Distribution functions in the statistical theory of turbulence. *Phys. Fluids* **10**, 969.

Moin, P., Adrian, R. J., Kim, J. (1987) Stochastic estimation of organized structures in turbulent channel flow, in: *Proc. 6th Turbulent Shear Flow Symp.*, Toulouse, 1987, 16.9.1-16.9.8.

Monin, A. S. (1967a) Equation for finite-dimensional probability distributions of turbulent field. *Dokl. Akad. Nauk SSSR* **177**, 1036-1038.

Nithianandan, C. K. (1980) Fluctuating velocity pressure field structure in a round jet turbulent mixing region. Ph.D. thesis, University of Illinois, Urbana, Illinois.

Novikov, E. A. (1967) Kinetic equations for vorticity field. *Dokl. Akad. Nauk. SSSR* **177**, 299-301.

Novikov, E. A. (1993) A new approach to the problem of turbulence, based on the conditionally averaged Navier-Stokes equations. *Fluid Dynamics Res.* **12**, 107-126.

Papoulis, A. (1984) *Probability, Random Variables and Stochastic Theory.* New York: McGraw-Hill.

Perry, A. E., and Chong, M. A. (1987) A description of eddying motions in flow patterns using critical-point concepts. *Ann. Rev. Fluid Mech.* **19**, 125-155.

Piomelli, U. (1987) Models for Large Eddy Simulations of Turbulent Channel Flows Including Transpiration. Ph.D. thesis, Stanford Univ., Stanford, California.

Robinson, S. K. (1991) Coherent motions in the turbulent boundary layer, *Ann. Rev. Fluid Mech.* **23**, 601-640.

Rogers, M. M., Moin, P. (1987) The structure of the vorticity field in homogeneous turbulent flows, *J. Fluid Mech.* **176**, 33.

Schumann, U. (1975) Subgrid scale model for finite difference simulations of turbulent flows in plant channels and annuli. J. *Comput. Phys.* **18**, 376-404.

Townsend, A. A. (1976) *The Structure of Turbulent Shear Flow*, 2nd Ed. Cambridge University Press, Cambridge.

Tung, A.T.C. and Adrian, R. J. (1980) Higher-order estimates of conditional eddies in isotropic turbulence. *Phys. Fluids* **23**, 1469-1470.

Tung, A. T. C. (1982) Properties of Conditional Eddies in Free Shear Flows. Ph.D. thesis, Univ. Illinois, Urbana, Illinois.

Ukeiley, L., Cole, D. R., Glauser, M. (1993) An examination of the axisymmetric jet mixing layer using coherent structure detection techniques. In: Bonnet, J. P., Glauser, M. N., Eds. *Eddy Structure Identification in Free Turbulent Shear Flows*. Dordrecht: Kluwer. 325-336.

Van Atta, C. W. and Chen, W. Y. (1968) Correlation measurements in grid turbulence using digital harmonic analysis. *J. Fluid Mech.* **34**, 497-515.

Willmarth, W. W., and Wooldridge, C. E. (1963) Measurements of the correlation between the fluctuating velocities and the fluctuating wall pressure in a thick turbulent boundary layer. AGARD Rep. 456.

Zhou, Z., Adrian, R. J., and Balachandar, S. (1995) Autogeneration of near-wall vortical structures in channel flow. Submitted to *Phys. Fluids.*

List of Recent TAM Reports

No.	Authors	Title	Date
714	Birnbaum, H. K., and P. Sofronis	Hydrogen-enhanced localized plasticity—A mechanism for hydrogen-related fracture	July 1993
715	Balachandar, S., and M. R. Malik	Inviscid instability of streamwise corner flow	July 1993
716	Sofronis, P.	Linearized hydrogen elasticity	July 1993
717	Nitzsche, V. R., and K. J. Hsia	Modeling of dislocation mobility controlled brittle-to-ductile transition	July 1993
718	Hsia, K. J., and A. S. Argon	Experimental study of the mechanisms of brittle-to-ductile transition of cleavage fracture in silicon single crystals	July 1993
719	Cherukuri, H. P., and T. G. Shawki	An energy-based localization theory: Part II—Effects of the diffusion, inertia and dissipation numbers	Aug. 1993
720	Aref, H., and S. W. Jones	Chaotic motion of a solid through ideal fluid	Aug. 1993
721	Stewart, D. S.	Lectures on detonation physics: Introduction to the theory of detonation shock dynamics	Aug. 1993
722	Lawrence, C. J., and R. Mei	Long-time behavior of the drag on a body in impulsive motion	Sept. 1993
723	Mei, R., J. F. Klausner, and C. J. Lawrence	A note on the history force on a spherical bubble at finite Reynolds number	Sept. 1993
724	Qi, Q., R. E. Johnson, and J. G. Harris	A re-examination of the boundary layer attenuation and acoustic streaming accompanying plane wave propagation in a circular tube	Sept. 1993
725	Turner, J. A., and R. L. Weaver	Radiative transfer of ultrasound	Sept. 1993
726	Yogeswaren, E. K., and J. G. Harris	A model of a confocal ultrasonic inspection system for interfaces	Sept. 1993
727	Yao, J., and D. S. Stewart	On the normal detonation shock velocity–curvature relationship for materials with large activation energy	Sept. 1993
728	Qi, Q.	Attenuated leaky Rayleigh waves	Oct. 1993
729	Sofronis, P., and H. K. Birnbaum	Mechanics of hydrogen–dislocation–impurity interactions: Part I—Increasing shear modulus	Oct. 1993
730	Hsia, K. J., Z. Suo, and W. Yang	Cleavage due to dislocation confinement in layered materials	Oct. 1993
731	Acharya, A., and T. G. Shawki	A second-deformation-gradient theory of plasticity	Oct. 1993
732	Michaleris, P., D. A. Tortorelli, and C. A. Vidal	Tangent operators and design sensitivity formulations for transient nonlinear coupled problems with applications to elasto-plasticity	Nov. 1993
733	Michaleris, P., D. A. Tortorelli, and C. A. Vidal	Analysis and optimization of weakly coupled thermo-elasto-plastic systems with applications to weldment design	Nov. 1993
734	Ford, D. K., and D. S. Stewart	Probabilistic modeling of propellant beds exposed to strong stimulus	Nov. 1993
735	Mei, R., R. J. Adrian, and T. J. Hanratty	Particle dispersion in isotropic turbulence under the influence of non-Stokesian drag and gravitational settling	Nov. 1993
736	Dey, N., D. F. Socie, and K. J. Hsia	Static and cyclic fatigue failure at high temperature in ceramics containing grain boundary viscous phase: Part I—Experiments	Nov. 1993
737	Dey, N., D. F. Socie, and K. J. Hsia	Static and cyclic fatigue failure at high temperature in ceramics containing grain boundary viscous phase: Part II—Modeling	Nov. 1993
738	Turner, J. A., and R. L. Weaver	Radiative transfer and multiple scattering of diffuse ultrasound in polycrystalline media	Nov. 1993
739	Qi, Q., and R. E. Johnson	Resin flows through a porous fiber collection in pultrusion processing	Dec. 1993

List of Recent TAM Reports (cont'd)

No.	Authors	Title	Date
740	Weaver, R. L., W. Sachse, and K. Y. Kim	Transient elastic waves in a transversely isotropic plate	Dec. 1993
741	Zhang, Y., and R. L. Weaver	Scattering from a thin random fluid layer	Dec. 1993
742	Weaver, R. L., and W. Sachse	Diffusion of ultrasound in a glass bead slurry	Dec. 1993
743	Sundermeyer, J. N., and R. L. Weaver	On crack identification and characterization in a beam by nonlinear vibration analysis	Dec. 1993
744	Li, L., and N. R. Sottos	Predictions of static displacements in 1–3 piezocomposites	Dec. 1993
745	Jones, S. W.	Chaotic advection and dispersion	Jan. 1994
746	Stewart, D. S., and J. Yao	Critical detonation shock curvature and failure dynamics: Developments in the theory of detonation shock dynamics	Feb. 1994
747	Mei, R., and R. J. Adrian	Effect of Reynolds-number-dependent turbulence structure on the dispersion of fluid and particles	Feb. 1994
748	Liu, Z.-C., R. J. Adrian, and T. J. Hanratty	Reynolds-number similarity of orthogonal decomposition of the outer layer of turbulent wall flow	Feb. 1994
749	Barnhart, D. H., R. J. Adrian, and G. C. Papen	Phase-conjugate holographic system for high-resolution particle image velocimetry	Feb. 1994
750	Qi, Q., W. D. O'Brien Jr., and J. G. Harris	The propagation of ultrasonic waves through a bubbly liquid into tissue: A linear analysis	March 1994
751	Mittal, R., and S. Balachandar	Direct numerical simulation of flow past elliptic cylinders	May 1994
752	Anderson, D. N., J. R. Dahlen, M. J. Danyluk, A. M. Dreyer, K. M. Durkin, J. J. Kriegsmann, J. T. McGonigle, and V. Tyagi	Thirty-first student symposium on engineering mechanics, J. W. Phillips, coord.	May 1994
753	Thoroddsen, S. T.	The failure of the Kolmogorov refined similarity hypothesis in fluid turbulence	May 1994
754	Turner, J. A., and R. L. Weaver	Time dependence of multiply scattered diffuse ultrasound in polycrystalline media	June 1994
755	Riahi, D. N.	Finite-amplitude thermal convection with spatially modulated boundary temperatures	June 1994
756	Riahi, D. N.	Renormalization group analysis for stratified turbulence	June 1994
757	Riahi, D. N.	Wave-packet convection in a porous layer with boundary imperfections	June 1994
758	Jog, C. S., and R. B. Haber	Stability of finite element models for distributed-parameter optimization and topology design	July 1994
759	Qi, Q., and G. J. Brereton	Mechanisms of removal of micron-sized particles by high-frequency ultrasonic waves	July 1994
760	Shawki, T. G.	On shear flow localization with traction-controlled boundaries	July 1994
761	Balachandar, S., D. A. Yuen, and D. M. Reuteler	High Rayleigh number convection at infinite Prandtl number with temperature-dependent viscosity	July 1994
762	Phillips, J. W.	Arthur Newell Talbot—Proceedings of a conference to honor TAM's first department head and his family	Aug. 1994
763	Man., C. S., and D. E. Carlson	On the traction problem of dead loading in linear elasticity with initial stress	Aug. 1994
764	Zhang, Y., and R. L. Weaver	Leaky Rayleigh wave scattering from elastic media with random microstructures	Aug. 1994
765	Cortese, T. A., and S. Balachandar	High-performance spectral simulation of turbulent flows in massively parallel machines with distributed memory	Aug. 1994

List of Recent TAM Reports (cont'd)

No.	*Authors*	*Title*	*Date*
766	Balachandar, S.	Signature of the transition zone in the tomographic results extracted through the eigenfunctions of the two-point correlation	Sept. 1994
767	Piomelli, U.	Large-eddy simulation of turbulent flows	Sept. 1994
768	Harris, J. G., D. A. Rebinsky, and G. R. Wickham	An integrated model of scattering from an imperfect interface	Sept. 1994
769	Hsia, K. J., and Z. Xu	The mathematical framework and an approximate solution of surface crack propagation under hydraulic pressure loading	Sept. 1994
770	Balachandar, S.	Two-point correlation and its eigen-decomposition for optimal characterization of mantle convection	Oct. 1994
771	Lufrano, J. M., and P. Sofronis	Numerical analysis of the interaction of solute hydrogen atoms with the stress field of a crack	Oct. 1994
772	Aref, H., and S. W. Jones	Motion of a solid body through ideal fluid	Oct. 1994
773	Stewart, D. S., T. Aslam, J. Yao, and J. B. Bdzil	Level-set techniques applied to unsteady detonation propagation	Oct. 1994
774	Mittal, R., and S. Balachandar	Effect of three-dimensionality on the lift and drag of circular and elliptic cylinders	Oct. 1994
775	Stewart, D. S., T. D. Aslam, and J. Yao	The evolution of detonation cells	Nov. 1994
776	Aref, H.	On the equilibrium and stability of a row of point vortices	Nov. 1994
777	Cherukuri, H. P., T. G. Shawki, and M. El-Raheb	An accurate finite-difference scheme for elastic wave propagation in a circular disk	Nov. 1994
778	Li, L., and N. R. Sottos	Improving hydrostatic performance of 1–3 piezocomposites	Dec. 1994
779	Phillips, J. W., D. L. de Camara, M. D. Lockwood, and W. C. C. Grebner	Strength of silicone breast implants	Jan. 1995
780	Xin, Y.-B., K. J. Hsia, and D. A. Lange	Quantitative characterization of the fracture surface of silicon single crystals by confocal microscopy	Jan. 1995
781	Yao, J., and D. S. Stewart	On the dynamics of multi-dimensional detonation	Jan. 1995
782	Riahi, D. N., and T. L. Sayre	Effect of rotation on the structure of a convecting mushy layer	Feb. 1995
783	Batchelor, G. K., and TAM faculty and students	A conversation with Professor George K. Batchelor	Feb. 1995
784	Sayre, T. L., and D. N. Riahi	Effect of rotation on flow instabilities during solidification of a binary alloy	Feb. 1995
785	Xin, Y.-B., and K. J. Hsia	A technique to generate straight surface cracks for studying the dislocation nucleation condition in brittle materials	March 1995
786	Riahi, D. N.	Finite bandwidth, long wavelength convection with boundary imperfections: Near-resonant wavelength excitation	March 1995
787	Turner, J. A., and R. L. Weaver	Average response of an infinite plate on a random foundation	March 1995
788	Weaver, R. L., and D. Sornette	The range of spectral correlations in pseudointegrable systems: GOE statistics in a rectangular membrane with a point scatterer	April 1995

List of Recent TAM Reports (cont'd)

No.	*Authors*	*Title*	*Date*
789	Anderson, K. F., M. B. Bishop, B. C. Case, S. R. McFarlin, J. M. Nowakowski, D. W. Peterson, C. V. Robertson, and C. E. Tsoukatos	Thirty-second student symposium on engineering mechanics, J. W. Phillips, coord.	April 1995
790	Figa, J., and C. J. Lawrence	Linear stability analysis of a gravity-driven Newtonian coating flow on a planar incline	May 1995
791	Figa, J., and C. J. Lawrence	Linear stability analysis of a gravity-driven viscosity-stratified Newtonian coating flow on a planar incline	May 1995
792	Cherukuri, H. P., and T. G. Shawki	On shear band nucleation and the finite propagation speed of thermal disturbances	May 1995
793	Harris, J. G.	Modeling scanned acoustic imaging of defects at solid interfaces	May 1995
794	Sottos, N. R., J. M. Ockers, and M. J. Swindeman	Thermoelastic properties of plain weave composites for multilayer circuit board applications	May 1995
795	Aref, H., and M. A. Stremler	On the motion of three point vortices in a periodic strip	June 1995
796	Barenblatt, G. I., and N. Goldenfeld	Does fully-developed turbulence exist? Reynolds number independence versus asymptotic covariance	June 1995
797	Aslam, T. D., J. B. Bdzil, and D. S. Stewart	Level set methods applied to modeling detonation shock dynamics	June 1995
798	Prasad N.B.R. and P. Sofronis	The effect of interface slip and diffusion on the creep strength of fiber and particulate composite materials	July 1995
799	Hsia, K. J., T.-L. Zhang, and D. F. Socie	Effect of crack surface morphology on the fracture behavior under mixed mode loading	July 1995
800	Adrian, R. J.	Stochastic estimation of the structure of turbulent fields	Aug. 1995